Inter-hemispheric synchronicity and symmetry: The functional connectivity consequences of stroke and neurodegenerative disease

Yuan Tao [a,*], Kyrana Tsapkini [a,b], Brenda Rapp [a,c,d]

[a] Department of Cognitive Science, Johns Hopkins University, Baltimore, MD 21218, USA
[b] Department of Neurology, Johns Hopkins School of Medicine, Baltimore, MD 21217, USA
[c] Department of Psychological and Brain Sciences, Johns Hopkins University, Baltimore, MD 21218, USA
[d] Department of Neuroscience, Johns Hopkins School of Medicine, Baltimore, MD 21218, USA

ARTICLE INFO

ABSTRACT

Stroke and neurodegenerative diseases differ along several dimensions, including their temporal trajectories -abrupt onset versus slow disease progression. Despite these differences, they can give rise to very similar cognitive impairments, such as specific forms of aphasia. What has been scarcely investigated, however, is the extent to which the underlying functional neuroplastic consequences are similar or different for these diseases. Here, for the first time, we directly compare changes in the brain's functional network connectivity, measured with resting-state fMRI, in stroke and progressive neurological disease. Specifically, we examined two groups of individuals with chronic post-stroke aphasia or non-fluent primary progressive aphasia, matched for their behavioral profiles and distribution of left-hemisphere damage. Using previous proposals regarding the neural functional connectivity (FC) phenotype of stroke as a starting point, we compared the two diseases in terms of homotopic FC, intra-hemispheric FC changes and also the symmetry of the FC patterns between the two hemispheres. We found, first, that progressive disease showed significantly higher levels of homotopic connectivity than neurotypical controls and, further, that stroke showed the reverse pattern. For both groups these effects were found to be behaviorally relevant. In addition, within the directly impacted left hemisphere, FC changes for the two diseases were significantly correlated. In contrast, in the right hemisphere, the FC changes differed markedly between the two groups, with the progressive disease group exhibiting rather symmetrical FC changes across the hemispheres whereas the post-stroke group showed asymmetrical FC changes across the hemispheres. These findings constitute novel evidence that the functional connectivity consequences of stroke and neurodegenerative disease can be very different despite similar behavioral outcomes and damage foci. Specifically, stroke may lead to greater independence of hemispheric responses, while neurodegenerative disease may produce more symmetrical changes across the hemispheres and more synchronized activity between the two hemispheres.

1. Introduction

Stroke and neurodegenerative disease differ in terms of several key neurological features and yet they can have remarkably similar cognitive/behavioral consequences (Ingram et al., 2020). This observation raises a number of questions about the neural consequences of the two diseases, including: Do stroke and neurodegenerative disease produce similar functional neuroplastic changes? Given the open-ended nature of this question and that fact that there have been no previous studies comparing these diseases, in this study, we use, as a starting point, the work of Siegel et al (Siegel et al., 2016) who, . on the basis of a large-scale investigation of inter and intra-hemispheric functional

---

connectivity patterns in sub-acute stroke, proposed a "general physiological network phenotype of stroke".[1] The proposed phenotype consisted of two key features: (a) decreased inter-hemispheric functional connectivity between homotopic regions and (b) increased intra-hemispheric functional connectivity between normally segregated functional networks in the ipsi-lesional hemisphere. In the work we report on here, we evaluate the hypothesis that stroke and neurodegenerative disease differ with regard to these network phenotypic features. This hypothesis is predicated on the assumption that, despite often producing similar cognitive/behavioral patterns, the different underlying neurological features of the two diseases, including their different temporal disease trajectories (abrupt onset versus gradual progression), may produce significantly different disease-specific neuroplastic changes. To examine the hypothesis of differential functional response patterns in stroke and neurodegenerative disease, we specifically evaluated functional connectivity in two groups of individuals with aphasia subsequent to stroke (post-stroke aphasia, PSA) and progressive neurological disease (non-fluent variant of primary progressive aphasia, PPA) who shared similar behavioral/cognitive profiles and distributions of left hemisphere damage.

1.1. Consequences of stroke and neurodegenerative disease for functional connectivity

The Siegel et al. (2016) stroke phenotype proposal was based on the analysis of resting-state fMRI data collected from a cohort of 100 individuals with sub-acute stroke and heterogenous behavioral deficits (including a subset of 33 individuals with aphasia). They examined interhemispheric homotopic functional connectivity (FC) as well as ipsi- and contra-lesional within and between network FC. In a previous study of FC in chronic post-stroke aphasia (PSA), Tao and Rapp (2020) found strong support for the claim of reduced inter-hemisphere homotopic FC, based on task-based background connectivity measures. The claim of reduced inter-hemispheric FC in PSA also found support in findings reported in Klingbeil et al. (2019). Furthermore, it is generally consistent with findings from research indicating that the two hemispheres may respond very differently in PSA (Anglade et al., 2014; Cao et al., 1999; Gainotti, 2015; Hartwigsen & Saur, 2019; Saur et al., 2006; Thulborn et al., 1999; Turkeltaub, 2015; Turkeltaub et al., 2011). However, with regard to the second proposed phenotype feature of increased intra-hemispheric FC, Tao and Rapp (2020) reported that that the patterns of intra-hemispheric FC in PSA that they observed were variable between and across functional networks and, therefore, that intra-hemispheric FC patterns defied a simple phenotypic characterization (see also Klingbeil et al., 2019).

With regard to primary progressive aphasia (PPA), the issues of FC lateralization and hemispheric symmetry or synchronization have not been previously directly examined. However, for non-fluent PPA, there are reports of FC changes in the right hemisphere that mirror those seen in the left hemisphere, despite the right hemisphere being relatively intact structurally (Mandelli et al., 2018; Tao et al., 2020), indirectly suggesting increased inter-hemispheric FC symmetry in PPA. If verified under direct examination, this pattern would be contrary to the results that have been reported for stroke. With regard to intra-hemispheric FC in PPA, both decreased and elevated FC have been found and there are both variant-specific and variant independent effects (Agosta et al., 2014; Bonakdarpour et al., 2019; Guo et al., 2013; Lehmann et al., 2015;

Mandelli et al., 2018; Tao et al., 2020; Whitwell et al., 2015). However, direct comparisons of intra-hemispheric FC in PSA and PPA using the same analysis approaches would be required in order to understand if and how these complex patterns are similar across these diseases.

1.2. Temporal dynamics of disease trajectory

Neurological conditions may differ along a number of dimensions with a salient one being their temporal trajectories, with some, such as stroke or hypoxia, typically having abrupt onsets while others, such as neurodegenerative diseases and slow-growing tumors, having a gradual progression. Although understanding the brain's neuroplastic responses to these temporal differences is of great interest, their effects have been scarcely investigated.

Previous research has provided clear evidence of the relevance of the temporal characteristics of lesion for overall recovery of function. Studies comparing behavioral recovery in rats subjected to successive resections varying in the number of stages and inter-lesion intervals have consistently shown that more gradual lesions were associated with better functional recovery (Patrissi & Stein, 1975; Stein et al., 1977). A review (Desmurget et al., 2007) of human studies of progressive damage (slow growing tumors) and acute damage (stroke) confirmed that gradually progressing damage generally yielded better cognitive outcomes and produced more neurotopographically distributed reorganization. These authors suggested that, with regard to the latter, progressive neurological diseases may parallel the effects of aging.

This investigation provides an opportunity to compare the consequences of diseases that vary starkly in terms of their temporal trajectories, and hence will shed light on the relevance of disease kinetics to functional neuroplasticity as well as on the possible relationship between FC patterns in neurodegenerative disease and aging. However, because the two diseases also differ along other dimensions that cannot be controlled, it will not be possible to definitely determine that the differences in temporal diseases trajectories are the source of FC differences that are documented. We return to these issues in the General Discussion.

1.3. The current study

Empirical and computational work has shown that, when subjected to damage, the human connectome undergoes a complex and dynamic series of neuroplastic changes. (Sale et al., 2015; Saur et al., 2006; Siegel et al., 2018; Stam et al., 2010; Tao et al., 2021; Tao & Rapp, 2019). While understanding the differential effects of different neurological diseases is clearly of great importance, inferences have been severely limited by enormous inter-study variability in neural measures and analytic approaches. To address this issue, we directly compared individuals with primary progressive aphasia (PPA, non-fluent variant) and post-stroke aphasia (PSA) who exhibited highly similar language phenotypes (see Ingram et al., 2020) and distributions of left-hemisphere damage. We specifically evaluated functional connectivity as indexed by the correlation of intrinsic brain activity (measured in task-free, resting-state fMRI) between pairs of brain regions. Using the Siegel et al. (2016) stroke phenotype proposal as a starting point, we examined functional connectivity (FC) changes in these two groups (compared to healthy controls) in terms of the two proposed stroke phenotype features. On that basis, in Analysis 1, we examined inter-hemispheric homotopic FC while, in Analysis 2a, we examined intra-hemisphere FC. In Analysis 2b, we carried out a more extensive evaluation of intra-hemispheric FC changes, directly comparing the FC changes of the two neuropathological groups with four different FC measures that evaluate functional integration/segregation at both global and local scales. Finally, in Analysis 3, we examined the degree of similarity in the patterns of intra-hemispheric FC changes between the two hemispheres, i.e., hemispheric symmetry, experienced by the two groups. The results of the full set of analyses provide novel evidence of

---

[1] Functional connectivity analyses serve to evaluate the strength of functional relationships between brain areas, with connectivity operationalized as the degree of correlation of neural activity between brain areas. Functional connectivity analyses, compared to approaches that evaluate mean activation or other functional characteristics of specific brain areas, provide a means for evaluating the degree to which different brain areas are integrated or segregated and how these relationships are affected by neurological disease.

both similar and different patterns of functional neuroplastic changes in the two groups, expanding our understanding of the possible phenotypic features of stroke and neurodegenerative disease.

2. Methods

2.1. Participants

Participants include 55 individuals with stroke or neurodegenerative disease and 41 healthy older controls. The neuropathological group included 25 individuals with post-stroke aphasia (PSA) who had suffered a single left-hemisphere stroke at least six months prior to the investigation. The PSA data used for this study were collected at the pre-treatment timepoint of a larger study of post-stroke language rehabilitation clinical trial (NCT01927302). Data of 30 individuals with non-fluent primary progressive aphasia (nfvPPA) were also collected at the pre-treatment timepoint from recruited for a clinical trial (NCT02606422). These participants were diagnosed with non-fluent PPA based on neuropsychological and language testing, structural MRI, and clinical assessment, according to consensus criteria (Gorno-Tempini et al., 2011) and had a history of progressive language deficits without primary memory deficits or other etiology (e.g., stroke, tumors, etc.). The two neuropathological groups were comparable in terms of years of education, gender, and aphasia profiles (Table 1). Participants in the PPA group tended to be older than those in the PSA group and, therefore, to verify that the results obtained were not due to age differences between the groups, we repeated all analyses between age-matched groups that excluded the 7 younger stroke participants and 13 younger controls (≤55 yo). Results obtained with these age-matched subgroups were comparable to those obtained with the full groups and are reported in Supplementary Materials 6. The study was approved by the Johns Hopkins Hospital and Johns Hopkins University Institutional Review Board. All participants provided informed consent.

2.2. MRI image acquisition

All MRI data were collected using a Phillips 3T scanner at the F.M. Kirby Research Center for Functional Brain Imaging (Baltimore, MD). Similar standard parameters for the resting-state fMRI and T1-weighted structural imaging were used across the groups. For the PPA group, the scanning protocol included one session of resting-state (8.75 min) and multiple structural scanning protocols, including T1-weighted structural imaging. The acquisition parameters for the rs-fMRI were as follows: TR: 2500 ms, TE: 30 ms, FOV: 240*141*240 mm (ap, fh, rl), flip angle 75 degrees, voxel dimension: 3*3*3 mm, data matrix: 80*80*47. The T1-weighted structural MRI acquisition parameters were as follows: TR: 8.1 ms, TE: 3.7 ms, FOV: 224*160*180 mm (ap, fh, rl), flip angle: 8 degrees, voxel dimension: 1*1*1 mm, data matrix: 224*224*160. For the PSA group, the protocol included two 7-minute runs of rs-fMRI carried out consecutively, with the following acquisition parameters: TR: 2400 ms, TE: 20 ms, FOV: 206*123*220 mm (ap, fh, rl), flip angle: 90 degrees, voxel dimension: 1.7*1.7*3 mm, data matrix: 128*128*41. The T1-weighted structural MRI acquisition parameters were as follows: TR: 6 ms, TE: 2.9 ms, FOV: 256*256*176 mm (ap, fh, rl), flip angle: 9 degrees, voxel dimension: 1*1*1 mm, data matrix: 256*256*176.

Twenty of the age-matched control participants were scanned with the PPA group's protocol and 21 with the PSA group's protocol and the two subgroups were combined to maximize sample size. However, we also repeated the analyses including the scanning protocol as a covariate and, despite this reduction in power, obtained comparable outcomes (see Supplementary Materials 7).

2.3. Quantifying structural damage

For each PPA and PSA participant, a summary statistic of the total amount of structural damage was calculated to examine whether

Table 1

Demographic information and language and cognitive assessment results. If different tests were administered to the PPA and PSA participants, the test names are presented as (PPA/PSA). Behavioral assessment results are presented as percentage accuracy unless otherwise noted. Standard deviation values are shown in parentheses. Norm values are shown in each cell in italics when available.

	PPA (n = 30)	PSA (n = 25)	Healthy Control (n = 41)
Age	68.8 (6.18)	66.56 (10.14)	60.61 (9.96)
Years of education	16.59 (2.55)	16.24 (1.8)	16.93 (2.77)
Gender (n of Female)	13	9	26
Time since onset (year)	3.66 (2.42)	6.6 (4.67)	NA
Lesion volume (cm^3)	NA	106 (70)	NA
Intracranial volume (%)	35.62 (2.83)	34.5 (3.26)	37.29 (2.29)
Clinical Dementia Rating (CDR, sum of boxes, total = 15)	4.91 (3.83)	NA	NA
Language and cognitive assessment (PPA and PSA only)			
Noun naming (BNT/ NNB)	74 (27) *<77 considered abnormal*[4]	52 (34) *99.87 (0.89)* [5]	
Verb naming (HANA/NNB)	68 (27) *<63 considered abnormal*[1]	70 (29) *99.74 (1.23)*[2]	
Semantic knowledge (PPT-short/PPT-long)	98 (5) *99 (2)*[6]	93 (6) *NA*	
Sentence comprehension (SOAP/NNB)	73 (18) *98 (1.04)*[7]	79 (16) *100 (0)*[1]	
Repetition (NACC-UDS sentence repetition/WAB-repetition)	78 (28) *NA*	72 (26) *98 (3)* [8]	
Spelling to dictation (NACC-UDS/PALPA40)	77 (24) *NA*	40 (25) *91 (NA)*	
Digit span forward (length of span/n of trials)	4.33 (1.48) *60–64 yo: 8.4 (1.9) 65–69 yo: 7.5 (2)*[9]	3.6 (1.65) *5 % percentile for 55–64 yo: 5*[10]	
Digit span backward (length of span/ n of trials)	3.03 (1.16) *60–64 yo: 6.5 (2) 65–69 yo: 6.3 (2.2)*[6]	2.36 (1.62) *7 % percentile for 55–64 yo: 3*[7]	
Spatial span (n of items)	3.83 (1.34) *NA*	4.72 (1.15) *NA*	
Trail Making Test A (time in second)	55.7 (21.59) *35.8 (11.9)*[6]	NA	
Trail Making Test B (time in second, max 300)	166.84 (89.45) *81.2 (38.5)*[6]	NA	
WABAQ	78.4 (20.7) *98.4 (1.0)*	NA	
Raven's progressive matrices	0.83 (0.11) *NA*	NA	

BNT: Boston Naming Test (Kaplan et al., 2001); NNB: Northwestern Naming Battery (Thompson et al., 2012); HANA: Hopkins Assessment of Naming Actions (Breining et al., 2021); PPT: Pyramid Palm Tree (Howard and Patterson, 1992); NACC-UDS: National Alzheimer's Coordinating Center Uniform Dataset (Staffaroni et al., 2021); SOAP (Love & Oster, 2002); WAB: Western Aphasia Battery (Kertesz, 2006); PALPA: Psycholinguistic Assessments of Language Processing in Aphasia (Kay et al., 1996).

[4] Breining et al., 2021.
[5] Thompson et al., 2012.
[6] Breining et al., 2014.
[7] Love and Oster 2002.
[8] Western Aphasia Battery. Kertesz, 2006.
[9] WAIS-III. Wechsler, D. (1997). WAIS-III Administration and scoring manual. San Antonio, TX: The Psychological Association.
[10] Wechsler Memory Scale (WMS) Wechsler, D. (1987). Wechsler Memory Scale—Revised. San Diego: The Psychological Corporation.

functional connectivity abnormalities identified in subsequent analyses were related to total structural damage. For each PPA participant, the total structural damage was indexed by the inverse of global gray matter volume calculated as the total gray matter volume divided by intracranial size using tissue segmentation results of FSL. For each PSA participant, as an index of structural damage we used the stroke lesion volume which was calculated as size of the lesion mask co-registered to standard MNI space. The lesion of each PSA participant was manually traced on their T1 images with T2-weighted FLAIR images used to improve tracing accuracy. These lesion masks were then co-registered into standard space using the transformation parameters calculated from the T1 images.

We also examined the spatial distribution of gray matter atrophy of the PPA group using voxel-based morphometry (VBM) analysis carried out with FSLVBM (Douaud et al., 2007) following the standard workflow. Specifically, the PPA group was compared to the 20 controls who were scanned with the same MPRAGE protocol as the PPA group (see *Participants*). Comparisons were conducted using a permutation-based voxel-wise GLM in FSLVBM with isotropic Gaussian kernel (sigma = 3 mm) spatial smoothing, including age and year of education as covariates. Voxel-wise results were corrected for multiple comparisons with threshold-free cluster enhancement (TFCE).

In addition, to consider possible effects of gray matter atrophy in the PSA group, we also evaluated gray matter volume in PSA using the same methods as were used with the PPA group described above, but excluding lesioned areas. Details of the VBM analysis are described in Supplementary Material 2. Anda global atrophy value was calculated for each PSA participant as the inverse of total gray matter volume divided by intracranial size using tissue segmentation results of FSL, with lesion volume excluded from both.

2.3.1. Resting-state functional MRI data pre-processing and connectome construction

2.3.1.1. Preprocessing. Resting-state fMRI data were preprocessed using FSL 5.0 as follows: motion correction with MCFLIRT, slice-timing correction, non-brain tissue removal with BET, spatial smoothing using a 5 mm FWHM Gaussian kernel, grand-mean intensity normalization, high-pass temporal filtering (0.01 Hz). In FSL, functional images were first registered to a subject's T1 image using boundary-based registration, then to standard MNI space. For the PSA participants, the stroke lesions were masked out during co-registration. A number of independent components were estimated by MELODIC in FSL to be used as confound variables when calculating FC (see the next section). Each participant's in-scanner motion was quantified by the root-mean-square (rms) value calculated by MCFLIRT and used as a confound variable in group comparisons.

2.3.1.2. Estimating functional connectivity (FC). For all analyses, functional connectivity (FC) was calculated using the preprocessed time-series co-registered to MNI space. The following confound variables were regressed out from the time-series: 12 motion parameters, averaged time-series of the white matter and the CSF segmented by FAST in FSL, and the first three MELODIC independent components that were identified as motion-related by AROMA (Pruim et al., 2015) together with visual inspection (see Supplementary Material 1 for summary of the MELODIC and AROMA results). FC values were then estimated with Pearson's correlation (with Fisher's z-transform). The functional connectomes across multiple runs for a participant were averaged. The analyses were conducted using the Python package *Nilearn* (https://nilearn.github.io).

Inter-hemispheric, homotopic FC (Analysis 1). For evaluating homotopic functional connectivity, we used the AICHA atlas (*Atlas of Intrinsic Homotopic Areas,* Joliot et al., 2015) that was specifically developed to study homotopic FC and included 174 pairs of homotopic

cortical parcels. For each PSA participant, voxels within the stroke lesion mask were excluded prior to calculating FC. Additionally, for each PSA participant, parcels with >75 % overlap with their lesion mask were excluded from subsequent statistical analyses. Across the 174 homotopic connections no individual connections were excluded from the statistical analyses, but for any given connection the number of excluded participants ranged from 0 to 12 (mean = 1.8+/-2.7), with the Rolandic Opercular Gyrus being the most lesioned. This resulting in only modest variability in degrees of freedom across connections.

Intra-hemisphere FC (Analysis 2). For these analyses, we constructed whole-brain connectomes using the Power atlas (Power et al., 2011) that consisted of 235 cortical 5 mm-radius nodes (subcortical and cerebellar nodes were excluded for the current study). For each participant, nodes with >50 % overlap with their lesion and/or CSF mask were excluded, resulting in 181–234 total nodes per individual in the PSA group and 224–235 for individuals in the PPA group. Note that as for the homotopic FC, all nodes were included in the group analysis with only the degrees of freedom varying slightly across the nodes.

Connectomes for evaluating the hemispheric symmetry of FC changes (Analysis 3). The analysis goal was to evaluate the degree to which the patterns of within-hemispheric FC changes, identified in Analysis 2, were similar (symmetrical) in the two hemispheres. However, since the Power atlas did not have a 1–1- correspondence of nodes in the two hemispheres, for each node in each hemisphere (from the Analysis 2 connectome), we generated a node at its mirror location in the opposite hemisphere, resulting in a connectome with a total of 235 pairs of symmetrical nodes. No nodes were excluded from the group analysis but after considering lesioned/atrophic tissue, there were a total of 357–469 nodes per individual in the PSA group and 445–470 for those in the PPA group.

2.4. Analysis 1: Comparison of the functional connectivity between homotopic regions for the PPA and PSA groups

Lower than normal homotopic FC has been shown to be a salient FC feature in stroke (Siegel et al., 2016; Tao & Rapp, 2020). Here we examined homotopic FC in the post-stroke aphasia (PSA) and PPA groups to investigate if PPA exhibited the same characteristics as PSA. First, we compared the average homotopic FC strength across all 174 cortical pairs of homotopic regions from the AICHA atlas between each neuropathological group and the control group. Second, for each neuropathological group, we characterized the spatial distribution of the homotopic FC changes across the brain by comparing the FC strength of each homotopic connection with those of healthy controls. Third, to examine the behavioral relevance of the homotopic FC changes, we evaluated their relationship with behavioral measures of language and executive functioning. For the latter analysis, we calculated an average homotopic FC change value for each participant in each group by averaging the FC change values for the abnormal homotopic connections identified from the previous step. As an overall indicator of language performance we used the language sub-score of the Clinical Dementia Rating (CDR, Knopman et al., 2008) for the PPA group and the WABAQ (Kertesz, 2006) for the PSA group. To index executive functioning, we used the Trail Making Test (A + B, *Army Individual Test Battery,* 1944) for the PPA group and the Raven's Progressive Matrices (Raven, 1941) for the PSA group, a test that heavily relies on working memory and cognitive control (Prabhakaran et al., 1997; Rao & Badeley, 2013; Sánchez-Cubillo et al., 2009). Additionally, we also examined more specific language tasks including naming, digit span forward and backward, and repetition.

The between-group comparisons were carried out with linear regression with Group as an independent variable and amount of in-scanner motion as the covariate. The connection-wise results were corrected for the 174 homotopic connections using the FDR correction (*alpha < 0.05*). For the evaluation of the relationship between homotopic FC changes and behavior, regression analyses were carried out in

which each participant's average FC strength was predicted by the behavioral scores of language and executive function tasks described above, with amount of structural damage and in-scanner motion included as covariates. The regression analyses were carried out with the *lm* function in R.

2.5. Analysis 2. Comparison of intra-hemisphere functional connectivity changes for the PPA and PSA groups

2.5.1. Analysis 2a. Connection-based comparisons

As discussed in the Introduction, higher than normal intra-hemisphere FC has been argued to be another phenotype feature of stroke (Siegel et al., 2016), though considerable variability across different intra-hemisphere connections has been reported. To examine this, we first conducted an analysis of all individual connections to obtain a panoramic view of the intra-hemisphere FC changes; we refer to this as a "connection-based" analysis. To do so, for each intra-hemispheric connection we compared FC strength for the PSA and PPA groups with the control group using independent t-tests. For the Power atlas, there are 6327 connections within the left-hemisphere, and 7625 within the right hemisphere. The results were FDR corrected for the total 13,952 connections (alpha < 0.05).

2.5.2. Analysis 2b. Nodal global and local properties

For a more in-depth comparison of the FC changes between the two neuropathological groups, we focused on nodal properties (i.e., FC properties of each brain region/node). We used nodal values, rather than connection-based values, because a nodal scale of data compression represents an intermediate level of granularity that preserves information for each brain region while also providing reasonable interpretability. For example, a nodal-based analysis allows one to see quite easily which regions are driving the dis/similarity between the two groups. Specifically, we examined four different nodal measures, two based on mean FC strength and two graph-theoretic measures, thus providing two measures of FC properties at both global and local scales.

2.6. Measuring nodal FC properties: Between- and within-network Mean-FC

First, for each node, we calculated its <u>mean-FC</u> strength as the average FC of its connections with other nodes. Moreover, as the resting-state functional connectome is known to consist of multiple functional networks, we separated each node's connections into *within-* and *between-network* connections based on a reference network organization identified with 38 older participants (>50 yo, mean age = 65+/-10) from a publicly available dataset NKI-Rockland (Nooner et al., 2012, see Supplementary Material 3 for details). As depicted in Fig. 1a, the reference organization consisted of 6 networks that we refer to, based on their neuroanatomical distribution, as: Occipital, Dorsal Frontoparietal (dFP), Perisylvian, Frontoparietal (FP), Temporal, and Default Mode Network (DMN). With the reference network, we calculated one global and one local <u>mean-FC</u> measure for each node: the *global, between-network* mean-FC value of a node corresponded to the mean FC of the connections between the node and every other node outside its own network (global FC); The *local, within-network* mean-FC value corresponded to the mean FC of a node's connections with all other nodes within its own network (local FC) (see Fig. S1 for a schematic illustration of the FC measures). Note that we calculated mean-FC strength values by averaging both positive and negative FC values. We did so because there is no clear consensus in the literature on the best approach for dealing with negative FC values and averaging is a very common approach. Additionally, this approach was consistent with the empirical observation that, in this data set, the negative FC values were overall lower in magnitude than the positive ones (for details, see SFig. 14).

2.7. Measuring nodal FC properties: Graph-theoretic measures

For each node, we also evaluated one global and one local <u>graph-theoretic measure</u>. *Global efficiency* (GE) is the inverse of the average *shortest path length* of a node (this is also known as *closeness*). A node that is functionally connected to all other nodes via only a few connections
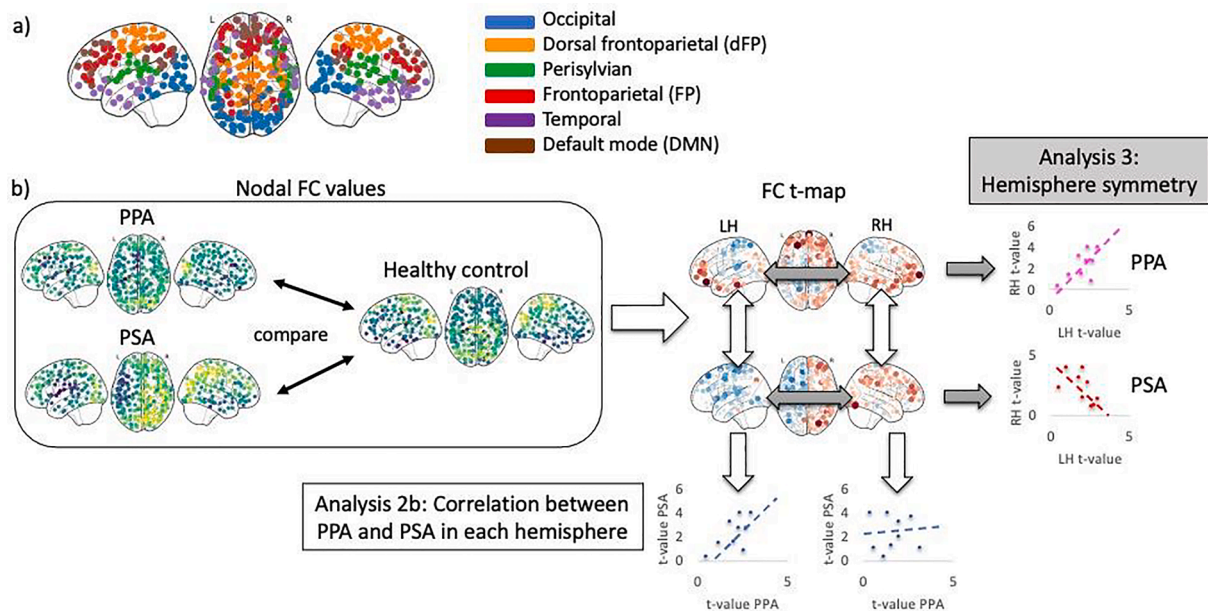

Fig. 1. The reference functional network organization and the analysis flow. (A) Six bilateral resting-state functional networks identified with an independent control group (see *Methods: Analysis 2b*). This served as the reference network organization used for calculating *between-/within*-network FC in subsequent analyses. (B) Analysis flow for the nodal measures. For comparing the FC changes between the two neuropathological groups (Analysis 2b) and for examining hemispheric symmetry of the two groups (Analysis 3), for each nodal measure, values from the PPA/PSA groups were first compared to the healthy controls to obtain a nodal *t*-map for each group that represented its FC changes relative to normal FC levels. Those nodal FC *t*-maps served as the bases for Analyses 2b and 3. A high correlation between the nodal t-values indicates that the two groups show high similarity in their FC changes (Analysis 2b) or that the two hemispheres have a high degree of symmetry (Analysis 3).

will have a low *average shortest path length* and hence a high GE value. *Clustering coefficient* (CC) is a local measure of a node's "cliqueness", such that a CC value of 1 indicates that all of the node's neighbors are also connected to each other (see Fig. S1 for a schematic illustration of the two graph-theoretic measures). Note that, unlike the mean FC measures described just above, both graph-theoretic measures are calculated independently of the reference network organization and, thus, can be considered to be "model free".

All graph-theoretic analyses were carried out with the Python-version of the *brain-connectivity-toolbox* (https://pypi.org/project/bctpy/). The graph-theoretic metrics were calculated at a series of proportional density threshold values (10 % to 40 % with 5 % increments) and binarized graphs were used to calculate each metric. For each node, the values obtained for the different density thresholds were then averaged before entering them into subsequent statistical analyses (Fornito et al., 2012). Because GE can be sensitive to differences in the numbers of nodes (van Wijk et al., 2010) across participants due to damage, we used *normalized GE* calculated relative to 10 random networks with preserved degree distribution (hereafter, we refer to it simply as GE). Since CC has not been shown to be sensitive to number of nodes (van Wijk et al., 2010) it was not normalized.

2.8. Comparison of within-hemisphere patterns of FC changes for the PPA and PSA groups

First, we calculated the FC changes for each neuropathological group by comparing their FC values to those of the control group. For each of the four measures described above, the nodal values of each neuro-pathological group were compared to the control group using linear regression with Group as an independent variable and amount of in-scanner motion as the covariate, generating a whole-brain, nodal *t*-map for each neuropathological group that represented differences between that group and the control group. We will refer to the differences in FC between each neuropathological group and the control group as **FC changes** and to the nodal *t*-maps that represent them as **FC-change maps.** We then examined how similar the two groups' overall FC changes were by correlating (Pearson's r) their FC-change maps within each hemisphere separately (See Fig. 1b for illustration of this analysis). These correlations were calculated for each of the four FC measures and their statistical significance was evaluated with 10 K permutation testing. Results were further Bonferroni corrected for the 8 comparisons (4 measures*2 hemispheres).

2.9. Analysis 3: Comparison of the hemispheric symmetry of FC changes for the PPA and PSA groups

Lastly, we examined the degree of similarity between the two hemispheres' FC changes for both the PPA and PSA groups. For each PPA and PSA participant, we calculated a *LH-RH change symmetry* score for each of the four FC measures as follows: For each node, we first computed its z-score against the control group value, then we correlated (Pearson's r) the z-scores between the 235 homologues nodes in the left and the right hemisphere to obtain a participant-specific *LH-RH change symmetry* score for each of the four FC measures (See Fig. 1b for illustration of this analysis). Scores for the PPA and PSA groups were compared with linear regression with Group as an independent variable and in-scanner motion included as a covariate. Results were Bonferroni corrected for the four FC measures.

Because the hemispheric *symmetry change score* values were based on the FC change values (i.e., z-scores), they indexed the symmetry of the FC changes relative to the neurotypical controls. In addition, therefore, we also examined the raw FC symmetry using the original nodal FC values for each participant and compared the values of each neuro-pathological group to the control group.

3. Results

3.1. Behavioral assessment

The results of comprehensive language and cognitive assessments are reported in Table 1. It is noteworthy that the two neuropathological groups presented with quite similar language deficit profiles. Namely, both groups showed moderate impairment in spoken naming, auditory sentence comprehension, repetition, spelling, while lexical semantic knowledge was relatively intact.

3.2. Structural damage

The PPA group exhibited the typical pattern of left hemisphere gray matter atrophy seen in non-fluent PPA involving primarily the posterior frontal and the anterior parietal lobes and the insula (Fig. 2). The structural damage of the PSA group (measured in terms of lesioned voxels) followed the typical pattern of MCA stroke with damage also concentrated in posterior frontal and parietal lobes and the insula (Fig. 2). The PSA group also showed some grey matter atrophy primarily in the cerebellum and in subcortical regions bilaterally (Fig. S2), and the gray matter atrophy (inverse of gray matter volume) in the RH showed a marginal relationship with lesion volume and (r = 0.3, p = 0.1) and a strong relationship with age (r = 0.53, p = 0.004).
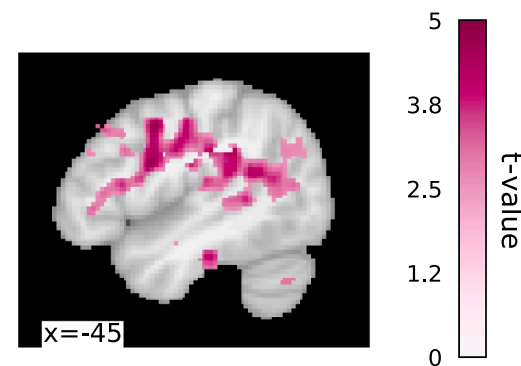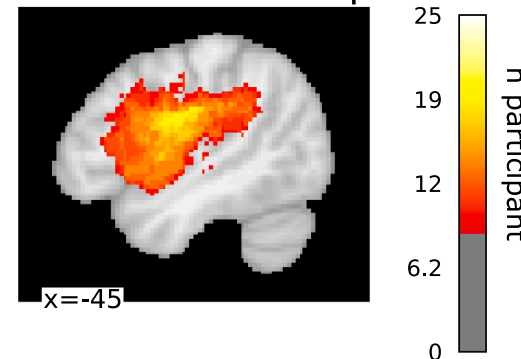

Fig. 2. Structural damage of the primary progressive aphasia (PPA, non-fluent variant) and the post-stroke aphasia (PSA) groups. Top: gray matter atrophy of the PPA group calculated by voxel-based morphometry analysis compared to the healthy controls. Whole-brain results were corrected with the Threshold-Free Cluster Enhancement method (corrected p < 0.01). Bottom: Lesion overlap of the 25 PSA participants, color scale indicates number of participants. Voxels that were damaged in more than one third of the group (n > 8) are shown.

3.3. Analysis 1: PPA and PSA showed different inter-hemispheric homotopic functional connectivity changes

The examination of the FC strength of 173 cortical homotopic pairs based on the AICHA atlas revealed that, on average, the PSA group's homotopic connectivity values were significantly lower than controls ($t = -4.42, p = 2.71e-5$) consistent with the "stroke phenotype" reported in previous studies (Klingbeil et al., 2019; Joshua Sarfaty Siegel et al., 2016; Tao & Rapp, 2020). Conversely, the PPA group showed higher homotopic FC values than the control group (PPA: $t = 3.9, p = 0.0002$; Fig. 3a). In other words, for the PSA group, activity across homotopic regions were less synchronized than in neurotypical controls and for the PPA group, the reverse pattern was observed. Furthermore, the distributions of abnormal homotopic FC connections were also very distinct for the two groups with a more widespread and more anterior distribution in PPA and a more posterior and lateral distribution in PSA (Fig. 3b).

To determine if these homotopic FC patterns had any behavioral relevance, we examined their relationship with behavioral measures. Because the two neuropathological groups were recruited for different studies, they shared few behavioral tests. We thought it could nonetheless be useful to consider two broad cognitive areas that were assessed in both groups (albeit with different specific tests): executive functioning and language. For the PPA group, who had overall higher-than-normal (elevated) homotopic FC values, for the significantly abnormal connections (shown in Fig. 3b), higher average homotopic FC values were found to be correlated with lower executive performance (longer Trail reaction times, $p = 0.0065$), but uncorrelated with language proficiency (CDR-language $p = 0.72$, Fig. 3c). Similar to the findings based on the CDR-language scores, scores from other language tasks (i.e., repetition, naming) were not correlated with the abnormal homotopic FC (see Supplementary Material 8). In contrast, for the PSA group, who had overall lower-than-normal homotopic FC values, for the significantly abnormal connections, higher average FC values were correlated with better language performance (WABAQ $p = 0.0077$) but were uncorrelated with executive functioning scores (Raven: $p = 0.52$, Fig. 3D). The other language tasks (i.e., repetition, naming) showed similar effects as the WABAQ (Supplementary Material 8). Additionally, the total amount of structural damage was uncorrelated with abnormal homotopic FC for either group (PPA atrophy: $p = 0.27$; PSA lesion volume: $p = 0.27$, atrophy of RH: $p = 0.27$). Detailed statistics of these analyses are reported in Supplementary Material 4.

In sum, although homotopic FC patterned in opposite directions for the two groups (abnormally high in PPA and abnormally low in PSA), for both groups better behavioral performance was associated with closer-to-normal levels of homotopic FC. Furthermore, the abnormal homotopic FC values showed behavioral relevance that was consistent with their anatomical distribution—medial frontal homotopic abnormalities in PPA were associated with executive processing performance and lateral temporal/parietal homotopic abnormalities in PSA were associated with language performance. The fact that these strikingly different FC patterns were associated with different cognitive functions in the two groups despite their overall similarity in terms of left hemisphere damage distribution and language profiles will be discussed in the General Discussion.

3.4. Analysis 2a. Intra-hemispheric functional connectivity changes in PPA and PSA

This analysis examined connection-based changes of intra-hemispheric FC for each neuropathological group. As depicted in Fig. 4, for both PPA and PSA, we observed both increased and decreased FC relative to the controls. For PPA, while there were many more connections with decreased compared to increased FC across the brain (286 vs 46), the numbers of decreased/increased connections were similar for the two hemispheres (decreased: 152 LH, 134 RH; increased: 46 LH,

61RH). The PSA group exhibited a more similar total number of increased and decreased connection (70 vs 51) but there was a striking hemispheric difference such that decreased FC connections were heavily concentrated in the left-hemisphere and increased FC connections were largely in the right-hemisphere (Fig. 4. decreased: 63 LH, 7 RH; increased: 19 LH, 32RH). Overall, these results do not provide clear support for the proposed "stroke phenotype" feature of increased ipsilesional FC, since for the PSA group the FC increases were concentrated in the RH and for the PPA group they are distributed similarly across both hemispheres. Furthermore, both groups also exhibited large numbers of connections with reduced FC values .

We also examined whether the abnormal intra-hemispheric FC values (separately analyzing the elevated and reduced values for each group) were related to the amount of structural damage in each hemisphere respectively. We found that, for PPA, the abnormal FC values were not related to amount of atrophy in either hemisphere (see Table S3). For PSA, we observed that reduced FC in the RH was related to greater RH atrophy ($r = -0.45$), and no significant correlations were found with lesion volume (see Table S3).

3.5. Analysis 2b. PPA and PSA groups show similar FC changes in the left but not the right hemisphere

As already indicated, for comparing the FC changes between the two neuropathological groups, we used nodal-level measures because this granularity offers better interpretability than connection-based values. Fig. 5 reports the unthresholded FC-change maps (t-value maps) for all four FC measures for the PPA and the PSA groups. Various patterns of between-group and between-hemisphere similarities in terms of FC changes are apparent from visual inspection, and these were then evaluated in the subsequent statistical analyses. For completeness, we also included visualizations of thresholded maps of the FC-change values in the Supplementary Materials (SFig. 15, FDR correction, alpha = 0.1).

3.6. Global connectivity: Between-network mean-FC and global efficiency (GE)

For global FC measures, the correlation of the t-values for the two neuropathological groups (differences from controls) revealed very different FC change patterns for the two hemispheres (Fig. 6a-b). In the LH, the values for both global FC measures were highly correlated across the groups (mean-FC: $r = 0.68$, corrected-$p < 0.0001$, GE: $r = 0.70$, corrected-$p < 0.0001$). In contrast the correlations for the two groups in the RH were significantly weaker for both measures (mean-FC: $r = 0.32$, corrected-$p = 0.0024$, LH vs RH $p = 0.0027$; GE: $r = 0.30$, corrected-$p = 0.0032$, LH vs RH $p = 0.0018$).

3.7. Local connectivity: Within-network FC and clustering coefficient (CC)

Analyses revealed that for mean within-network FC, as reported above for global connectivity and between network mean FC, changes in the LH of the two groups were significantly and positively correlated whereas the RH values were not (LH: $r = 0.40$, corrected-$p < 0.0001$; RH: $r = 0.02$, corrected-$p > 1$, LH vs RH: $p = 0.0021$. Fig. 6). For the graph-theoretic measure CC, the two groups' values were significantly positively correlated in both the LH and RH and there was no significant difference between the hemispheric values (LH: $r = 0.41$, corrected-$p < 0.0001$: RH: $r = 0.38$, corrected-$p < 0.0001 = 0.0024$, LH vs RH: $p = 0.42$).

In sum, for three of the four nodal measures we examined, PPA and PSA groups showed significantly more similar FC changes in the LH than in the RH. The results indicated that individuals with PPA and PSA underwent quite similar FC changes in the LH, whereas in the relatively intact RH, the FC changes of the two groups diverged.
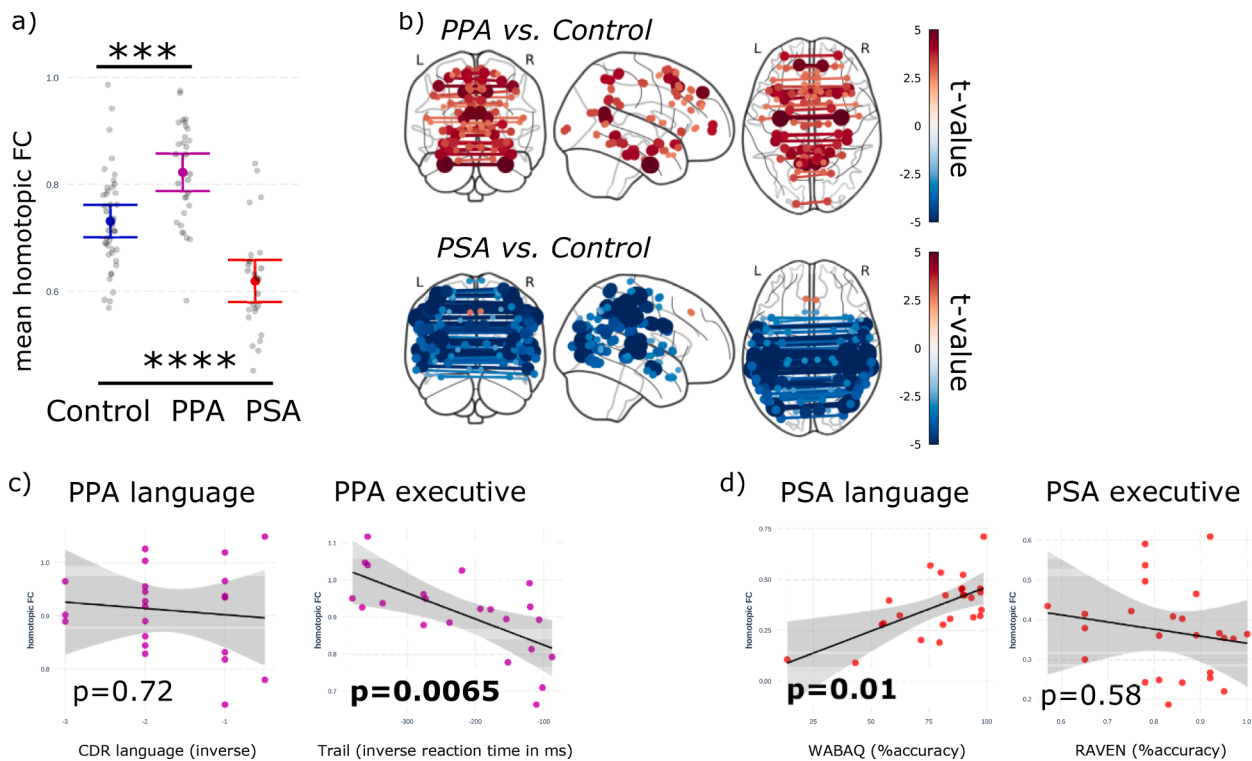
Fig. 3. Inter-hemispheric homotopic functional connectivity changes for the two neuropathological groups (Analysis 1). (A) Average homotopic FC strength across the173 homotopic connections from the AICHA atlas (Joliot et al., 2015). Relative to the healthy control group, values for the PPA group were significantly higher, while PSA values were significantly lower. ****:p < 0.0001, ***:p < 0.001 (B) PSA and PPA group comparisons with FC values for each homotopic connection. Significant effects are depicted (FDR corrected, alpha < 0.05). Positive t-values indicate PPA/PSA group values that were greater than those of the control group (red) and negative t-values (blue) indicate PPA/PSA group values that were lower than those of the control group. Node size and edge thickness are proportional to the t-values. For the PPA and PSA groups, not only were the FC changes in opposite directions but, furthermore, the two groups also exhibited different neurotopographic distributions of their abnormal homotopic connections. (C) Relationship between homotopic FC (average values per participant across all significant homotopic connections) and behavioral scores for the PPA group. Left: CDR-language (Knopman et al., 2008), x-axis indicates inverse severity score (i.e., higher values indicate better language performance). Left: Executive function as measured by Trail Making Test (A + B), x-axis indicates inverse reaction time in millisecond (i.e., higher values, faster reaction time - better performance); (D) Relationship between homotopic FC (average values per participant across all significant homotopic connections) and behavioral scores for the PSA group. Left: Overall language performance measured by WAB-AQ (Kertesz, 2006). Right: Executive function measured by Raven's Progressive Matrices (Raven, 1938). For both tests, higher values indicate better performance. (For interpretation of the references to color in this figure legend, the reader is referred to the web version of this article.)
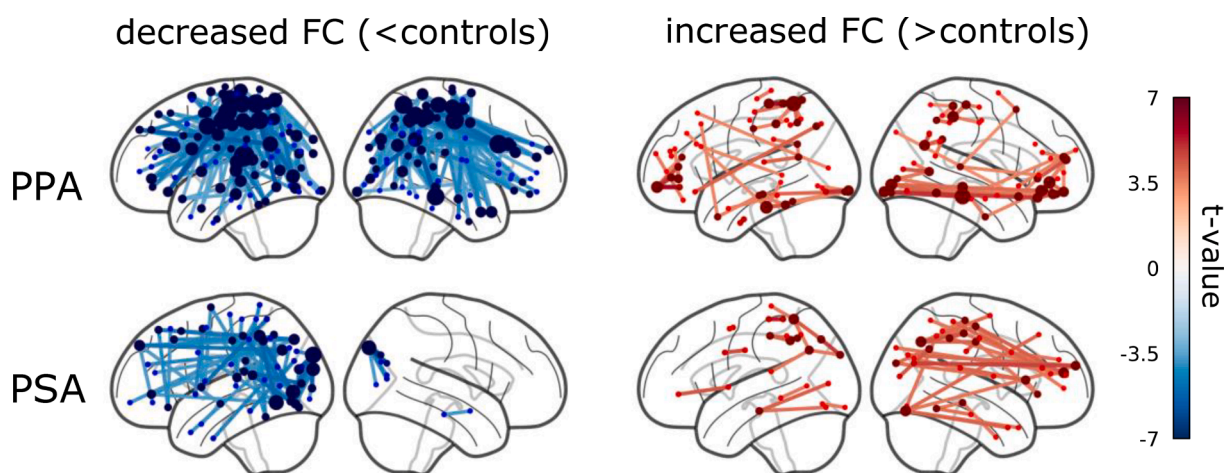

Fig. 4. Intra-hemisphere, connection-wise functional connectivity (FC) changes of the PPA (top) and the PSA group (bottom). Significant effects are depicted (FDR corrected, alpha < 0.05) and the decreased (blue, negative t-values against controls) and increased connections (red, positive t-values against controls) are showed separately. Node size is proportional to the node's (absolute) t-value sum. (For interpretation of the references to color in this figure legend, the reader is referred to the web version of this article.)
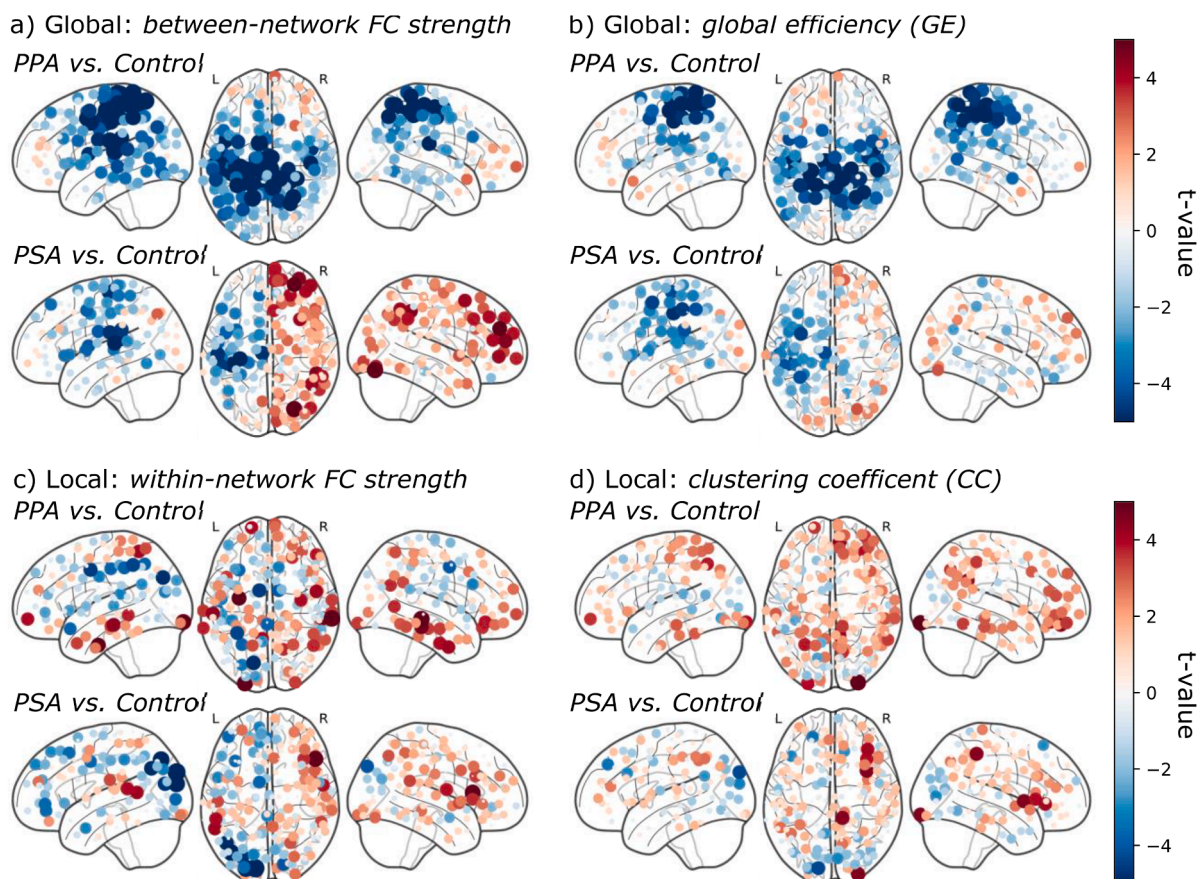
a) Global: *between-network FC strength*
PPA vs. Control

b) Global: *global efficiency (GE)*
PPA vs. Control

PSA vs. Control

PSA vs. Control

c) Local: *within-network FC strength*
PPA vs. Control

d) Local: *clustering coefficent (CC)*
PPA vs. Control

PSA vs. Control

PSA vs. Control

Fig. 5. FC-change maps for the four FC measures examined. Nodes correspond to those in the Power atlas (Power et al., 2011) and results are depicted on a glass brain. Color scale indicates *t*-values comparing PPA/PSA groups to the control group on each the four FC measures. Positive values (red) indicate PPA/PSA group values were greater than the control group and negative values (blue) indicate they were lower than control values. (A)-(B): *T*-value maps of the PPA/PSA groups vs controls for the global connectivity measures of mean *between-network* FC and *global efficiency* (GE); (C)-(D) *T*-value maps of PPA/PSA groups vs controls for the local connectivity measures of mean *within-network* FC and *clustering coefficient* (CC). (For interpretation of the references to color in this figure legend, the reader is referred to the web version of this article.)

3.8. Analysis 3. Hemispheric FC symmetry: The PPA group showed greater symmetry than the PSA group

In this analysis, we evaluated the hemispheric symmetry of the FC changes, i.e., the extent to which changes in the two hemispheres mirrored each other in PPA and PSA. The analysis results show that, for each of the four FC measures, *LH-RH change symmetry scores*, calculated from nodal z-scores for each participant, were significantly higher for the PPA than the PSA group (Fig. 7. *Bonferroni corrected p-values: Global: between-network FC: corrected-p = 0.0024; GE: corrected-p = 2.8e-06; Local: within-network FC: corrected-p = 4.2e-5; CC: corrected-p = 0.0008*). In addition, these symmetry scores were not related to the extent of total structural damage (*Global: between-network FC: PPA r = 0.13, p = 0.49, PSA lesion r = 0.11, p = 0.61, PSA atrophy: r = 0.05, p = 0.81; GE: PPA r = 0.1, p = 0.6, PSA r = 0.09, p = 0.68, PSA atrophy: r = 0.05, p = 0.8; Local: within-network FC: PPA r = 0.11, p = 0.57, PSA r = 0.22, p = 0.29, PSA atrophy: r = 0.17, p = 0.42; CC: PPA r = −0.04, p = 0.84, PSA r = 0.17, p = 0.41, PSA atrophy: r = 0.18, p = 0.38. p-values not corrected*). In sum, the PPA group showed more symmetrical FC changes than did the PSA group.

Given that the hemispheric *change score* values were based on the FC change values (i.e., z-scores) and, hence, indexed the symmetry of the FC changes relative to control values, we also examined *raw* FC symmetry using the original nodal FC values for each participant (including the controls). We found, that as with the FC*change scores*, the PPA group also showed higher raw LH-RH similarity than the PSA group across all four FC measures (Fig. S4). When compared to the controls, the PPA group

generally exhibited higher than normal FC symmetry and the PSA exhibited lower than normal FC symmetry (numerically and/or statistically). The results are reported in Supplementary Material 5.

4. Discussion

To better understand the consequences of stroke and progressive brain disease for the brain's functional reorganization and neuroplastic responses, we examined the functional network organization of two groups of individuals, one with primary progressive aphasia (PPA, non-fluent variant) and another with post-stroke aphasia (PSA). More specifically, we set out to evaluate the hypothesis that the two diseases may differ with regard to two stroke phenotype features proposed in Siegel et al (2016): decreased inter-hemispheric and increased intra-hemispheric functional connectivity (FC). In order to be in a position to draw stronger inferences about the contribution of disease type to any observed FC changes, we selected groups that were well matched in terms of locus of neuroanatomical damage (left frontal and anterior parietal lobe, Fig. 2) and aphasia profiles (Table 1). Using resting-state fMRI, we examined four FC properties, two each at global and local network scales. Our key findings were as follows: (1) With regard to inter-hemispheric homotopic FC (hemispheric synchronization), the PSA group exhibited lower than normal levels, consistent with the Seigel et al. phenotype feature, whereas the PPA group exhibited higher than normal FC between homotopic areas. These changes were found to be associated with different behavioral patterns (Fig. 3). (2) With regard to intra-hemispheric FC, in the primarily damaged left hemisphere, both
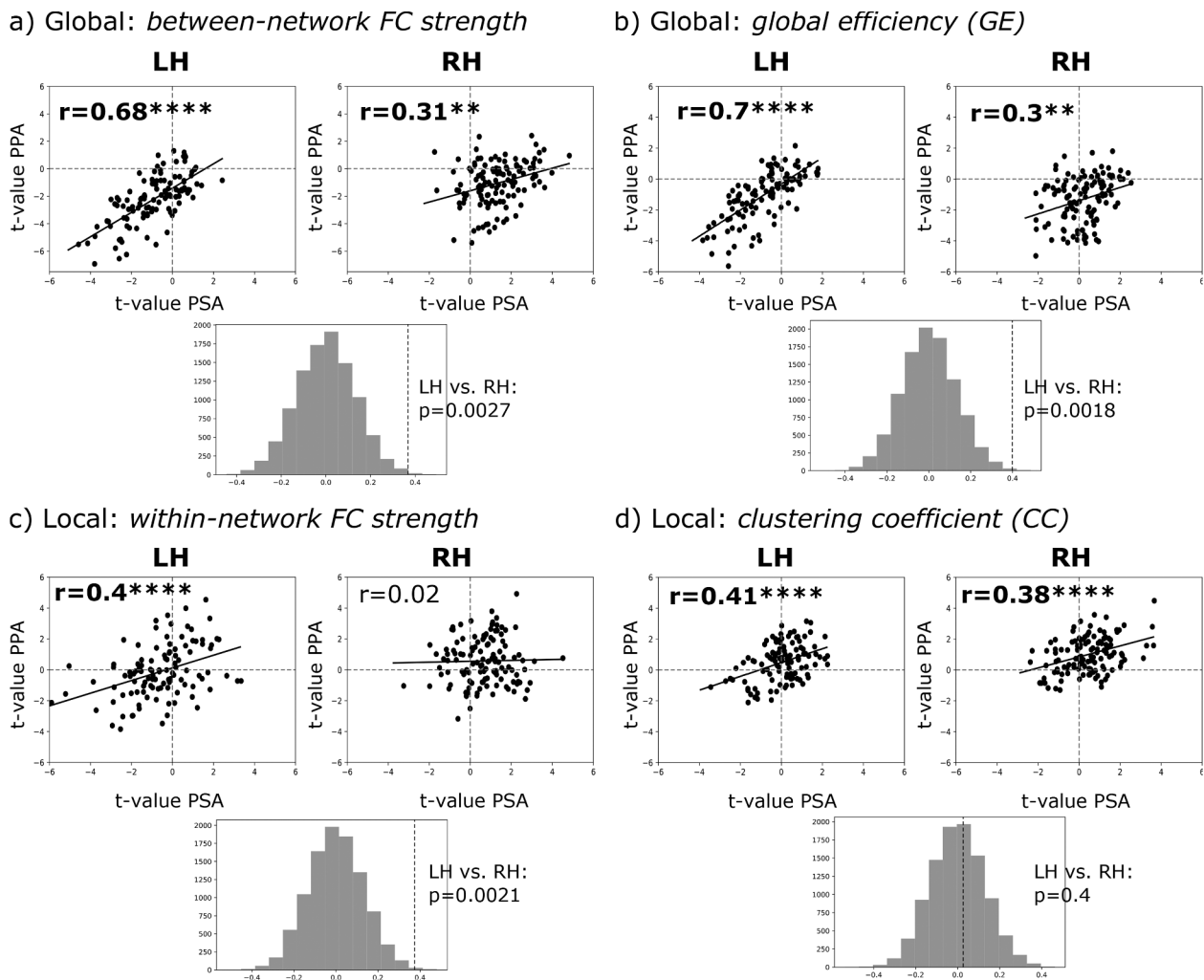
Fig. 6. Comparison of the two neuropathological groups in terms of intra-hemispheric FC changes. For each hemisphere and each of the four FC measures, each scatterplot represents the correlation between PSA and PPA groups of their nodal *t*-values (that index each node's FC change relative to the control group). Note that these nodal *t*-values are the same values as reported in Fig. 5. A high correlation value indicates highly similar nodal FC changes for the two groups, for a given hemisphere. The four histograms represent the results of the permutation tests evaluating the differences between the left and right hemisphere correlation values, for each of the four FC measures. Each histogram corresponds to the null distribution of differences between the LH and RH correlation values obtained from 10 K permutation test based on random shuffling of nodes across hemispheres. Dashed lines indicate the observed difference between the left and right hemisphere correlation values. (A)-(B) For each hemisphere, the correlation between PPA and PSA groups of nodal *t*-values for *between-network* mean-FC and *global efficiency* (GE). (C)-(D) For each hemisphere, the correlation between PPA and PSA groups of nodal *t*-values for *within-network* mean-FC and *clustering coefficient* (CC). Permutation testing shows that, for all FC measures except for CC, the correlation of FC values between the two groups in the LH was significantly higher than in the RH. ***:p < 0.01, ****:p < 1e-4 after Bonferroni correction.*

groups showed complex patterns of FC increases and decreases (Fig. 4) which, nonetheless, were highly correlated across the two groups for all the four FC measures (Figs. 5 and 6). In contrast, in the relatively intact right hemisphere, the two groups showed distinct FC change patterns with the PPA group exhibiting FC changes that mirrored those in the left-hemisphere, whereas PSA exhibited a markedly different pattern of FC changes in the right hemisphere compared to the left (Figs. 5 and 6); (3) Importantly, across all four FC measures, the PPA group showed significantly more symmetrical changes across the two hemispheres compared to the PSA group (Fig. 7). Together, the results reveal similar FC properties in the heavily damaged left hemisphere for both stroke and progressive aphasia. Otherwise, despite similar language profiles and damage distributions, the two groups exhibited distinctive patterns of inter-hemispheric FC symmetry and synchronization,

4.1. Functional connectivity between the hemispheres (hemispheric synchronization)

Homotopic FC measures the degree to which the fMRI time-courses of homologous brain regions of the two hemispheres are correlated and, thus, can be seen as reflecting the degree of synchronization (or integration) between homologous brain regions of the two hemispheres. Siegel et al. (2016) proposed that a decrease in homotopic FC was a key phenotypic feature of stroke. In the current study, our finding of significantly lower than normal homotopic FC for the PSA group (Fig. 3) provides further support for the claim. The current findings are also consistent with those we reported in Tao & Rapp (2020). While the previous study and the current one involved a largely overlapping set of PSA individuals, the neural measures were entirely different. Tao & Rapp (2020) analyzed background connectivity extracted from task-based BOLD obtained while participants were carrying out a spelling task in the scanner while, in the present study, resting-state BOLD was analyzed. The finding of similar results with different neural measures
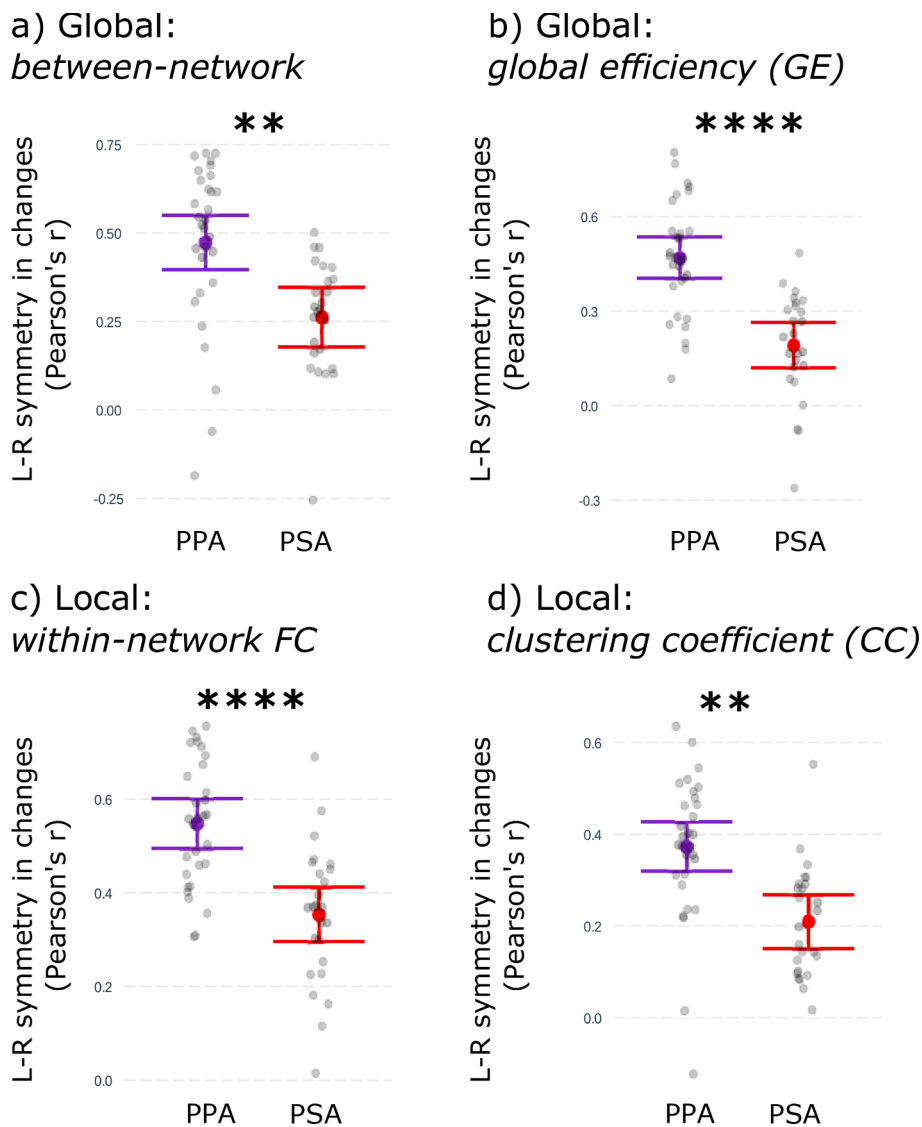
a) Global:
between-network

b) Global:
global efficiency (GE)

c) Local:
within-network FC

d) Local:
clustering coefficient (CC)

Fig. 7. Hemispheric symmetry of intra-hemispheric FC changes (relative to controls) for PPA and PSA (Analysis 3). LH-RH symmetry scores were calculated using nodal z-scores for each participant (see text for details) and values between the two neuropathological groups were compared. (A)-(B) LH-RH symmetry in global connectivity changes measured by mean *between-network* FC and *global efficiency* (GE). (C)-(D) LH-RH symmetry in local connectivity changes measured by mean *within-network* FC and *clustering coefficient* (CC). Across all the measures, the PPA group showed significantly greater similarity across the hemispheres than the PSA group, indicating that the FC changes (relative to controls) for the PPA group were more symmetrical between the two hemispheres than for the PSA group. **:$p < 0.01$, ***$p < 0.001$, ****$p < 0.0001$, after Bonferroni correction.

and different stroke groups at both sub-acute and chronic stages strengthens the claim that decreased homotopic FC may well be a characteristic feature of stroke.

Importantly, the analyses revealed opposite patterns in PSA and PPA, with the PPA group exhibiting a significant increase in homotopic FC relative to controls that was also significantly higher than that observed in the PSA group (Fig. 3). Thus, the two neurological diseases resulted in highly distinctive FC changes with regard to the synchronization of resting-state activity across homologues areas. This is consistent with our prediction that the two diseases would differ regarding fundamental FC features, despite the overall similarity of the groups in terms of language profiles and damage distribution.

The behavioral relevance of these homotopic FC changes was supported by their significant association with behavioral measures. For the PSA group, which showed lower than normal homotopic FC, lower FC values were associated with lower language scores (Fig. 3d). For the PPA group, which exhibited higher than normal homotopic FC, higher FC values were associated with worse executive performance (Fig. 3c). In sum, for both groups, more abnormal homotopic FC values (either elevated or reduced) were related to worse behavioral scores. Of further interest is the fact that the two groups showed complementary patterns: for the PSA group the homotopic FC changes were unrelated to executive function scores, while for the PPA group they were unrelated to

language scores.[2] This complementary pattern of association between homotopic FC changes and behavior is likely related to the different neurotopographical distributions of the significant homotopic FC changes, namely, the PPA group exhibited a largely medial and anterior distribution of elevated homotopic FC, while the PSA group's reduced homotopic levels were concentrated in lateral temporal and posterior areas (Fig. 3b). In other words, behavioral performance was linked to FC changes in brain areas associated with the correlated cognitive functions such that executive function performance was associated with homotopic FC changes in the medial/anterior regions that are often associated with executive functions, while language performance was linked to homotopic FC changes involving (temporal and parietal) language-

---

[2] While we acknowledge that it would have been preferable for both groups to have been tested on the same language and executive function tasks, that was not possible given that the data were collected from different studies. Nonetheless, we would note that as researchers we typically draw inferences across studies that do not use the same tasks. In other words, we assume that inferences about language and executive functions can be valid across a range of tasks measuring these skills.

related areas.[3] Note that despite contrasting overall patterns of elevated and depressed homotopic FC in the two groups, a few connections were identified with reduced homotopic FC in the PPA group when scanning protocol was included as a co-variate (supplementary analyses, SFig. 10), and a small number of connections were identified with elevated homotopic FC in the PSA group (Fig. 3b, also SFig. 6, 10). Thus, there may exist a small number of homotopic connections with values that are different from the overall patterns. It is likely that specific cohort characteristics (e.g., lesion size and location, disease progression) play a role in whether these values emerge as statistically significant in any given sample. It will be useful for future research to examine the homotopic FC patterns in each group in more detail as any variability may constitute a source of information regarding underlying neuro-physiological mechanisms.

4.2. Similar patterns of left-hemisphere FC changes

The second stroke phenotype feature proposed by Siegel et al (2016) was increased FC between ipsi-lesional functional networks. In that regard it is worth noting that Tao & Rapp (2020) already reported a complex pattern of ipsi-lesional left hemisphere FC changes in the stroke group they studied and pointed out that even Siegel et al (2016) had not reported a consistent FC pattern in the ipsi-lesional hemisphere. In fact, the significant result Siegel et al. reported was limited to the FC between the dorsal attention network and the default mode network. Thus, this second proposed stroke phenotype feature had already not received strong support, something we confirmed in the current study.

We found a complex picture that included both FC increases and decreases in the left hemisphere (Fig. 4). Both groups actually exhibited an overall decrease in left hemisphere FC, although there were also a small number of statistically significant FC increases as well. What was most salient, however, was the similarity of the left-hemisphere FC change patterns for the two groups (Figs. 5 and 6). In fact, for the four nodal FC measures, at both local and global scales, there were strong and highly significant correlations between nodal FC values across the two groups (r values ranged from 0.4 − 0.7) in the heavily damaged left-hemisphere. This similarity of the left-hemisphere FC profiles across the groups seems to suggest (at least for these FC measures) that the different characteristics of the two diseases (e.g., the nature of the structural damage and the disease trajectories) may not have been highly relevant in the left hemisphere and that, instead, the **location** of damage (regardless of its etiology) was the primary driver of the neuroplastic FC changes we observed. Note that we also found that the overall magnitude of structural damage (global gray matter atrophy and lesion volume for PPA and PSA, respectively) was not a significant predictor of the left-hemisphere FC changes (Supplementary Material 4).

4.3. Different patterns of right-hemisphere FC changes

The original stroke phenotype study (Siegel et al., 2016) did not

report significant FC effects in the contralesional hemisphere in their analysis of post-stroke FC changes. However, it is worth noting that their sample was extremely heterogenous and included individuals with either left or right hemisphere stroke at the subacute stage (<2 weeks). In contrast, the current investigation that involved only chronic (>6 months) left hemisphere stroke and a more behaviorally homogeneous population. Here we found that both PPA and PSA groups exhibited significant FC changes in the right hemisphere (Fig. 4). For the PSA group these consisted almost entirely of FC increases relative to controls, while for the PPA group the right hemisphere changes consisted primarily of FC decreases. Furthermore, even the FC increases were distributed quite differently for the two groups, as they were concentrated in ventral regions in PPA and primarily in dorsal areas in PSA. Thus, in contrast to the strong similarity of the FC changes for the two groups in the left hemisphere, the two groups exhibited quite different patterns of FC changes in the right hemisphere (see Figs. 5 and 6). The contrast between the two hemispheres in terms of between-group similarity is captured quantitatively by the finding that for three of the four FC measures (all except CC) the correlations of FC changes between the two groups were significantly lower in the right hemisphere than in the left (Fig. 6).

A key question concerns the cause of these right hemisphere differences between the two groups. One possibility to consider is that the FC changes in the RH are driven by different degrees of structural damage in the RH. However, we did not find that the FC changes in the RH were related to the extent of structural damage except for the finding that for the PSA group, reduced RH FC was moderately related to greater RH atrophy (r = -0.45, uncorrected p = 0.03, see Table S3), and the same trend was also evident in the PPA group (r = -0.3, uncorrected p = 0.11, see Table S3). Thus, the divergent RH FC patterns of the two groups are not readily explained by differences between the groups with regard to structural damage. This suggests an alternative account, raising the possibility that the divergence between the two groups in terms of FC patterns could have been driven by differences in the time-course of the two diseases that may have resulted in different patterns of functional reorganization. This is a hypothesis that would especially benefit from longitudinal empirical studies as well as computer simulation work.

4.4. Differences in the inter-hemispheric symmetry of FC changes

The differences between the PSA and PPA groups with regard to the functional synchronization of the homotopic regions described above (i. e., homotopic FC, Fig. 3), imply that the two groups also differ in the degree to which changes in one hemisphere mirrored those in the other (i.e., hemispheric symmetry). The question of hemispheric symmetry of FC changes was examined in more detail in Analysis 3 which went beyond examining connectivity between homologous areas, to a more comprehensive examination of multiple measures of FC changes within each hemisphere in order to examine the degree to which changes in one hemisphere were reflected in the other. This detailed analysis of hemispheric FC symmetry revealed that across all four FC measures, the FC changes exhibited by the PPA group were significantly more similar across the hemispheres than they were for the PSA group (Fig. 7). In other words, the PPA group experienced more symmetrical FC changes than did the PPA group. Moreover, we found no statistically significant correlations between the degree of FC symmetry and the extent of structural damage (Analysis 3). The finding of robust differences in the hemispheric symmetry of FC changes between the two groups may well represent the most significant contribution of this work to our understanding of the characteristic (or phenotypic) FC responses of the brain to these different neurological diseases.

4.5. Differences in hemispheric symmetry and synchronization: Underlying mechanisms?

Stroke and progressive neurological disease differ along various

---

[3] We note that while it is true that some values for the PSA group were excluded from analysis (parcels of a participant if>75% of the parcel is damaged), and hence some parcels have a lower degree of freedom for the PSA group, it is very unlikely that this complementary pattern between PSA and PPA was due to greater exclusion of participants from the analysis anterior nodes due to the primarily anterior lesions of the PSA group, for the following reasons: 1) No parcels were completely excluded from the analysis, instead individual participant values were excluded for the PSA group. The participant level exclusion could introduce lower statistical power (decreased sample size) in the results which would be unlikely to increase the probability of significant effects; 2) the PSA group's most lesioned areas (i.e., MCA territory) and the regions that had elevated levels of FC in the PPA group do not overlap. In other words, the regions shat showed elevated FC in the PPA group did not have decreased statistical power due to missing data-points in the PSA group. Thus, this is an unlikely explanation for the group differences we observed.

dimensions making it extremely difficult to determine which dimension/s is/are responsible for both the similarities and differences in the neuroplastic responses we have reported for the two groups. Despite this difficulty, the issue is of fundamental importance and, therefore, merits some discussion. Here we bring together the relevant evidence (albeit limited) from this investigation regarding the nature of the structural damage, the location of the structural damage and the temporal trajectories of the diseases.

Nature of the structural damage. Compared to progressive neurological disease, stroke clearly produces a more severe focal structural disruption to the brain, directly destroying contiguous regions of gray matter and often creating white matter disconnections. Particularly in the chronic stage it can additionally produce diffuse gray and white matter atrophy (Brodtmann et al., 2020; Crofts et al., 2011; Egorova-Brumley et al., 2022). In contrast, in progressive neurological disease, although damage is typically concentrated in a disease "epicenter" (Gorno-Tempini et al., 2011; Rogalski et al., 2011), damage is more diffuse than in stroke even within highly affected regions as these areas are typically not fully destroyed but continue to contain neurons and their connections. While we are not in a position to draw strong conclusions about the contribution of these differences in the nature of the structural damage to the FC differences we have reported, we believe that it is worthwhile to review some of the potentially relevant evidence from this study.

First, in various analyses we evaluated the contribution of the magnitude of damage to the FC patterns we have observed. For PPA, the magnitude of structural damage was quantified as gray matter atrophy, and for PSA it was quantified as the stroke infarct (and we also considered atrophy volume for PSA). The rationale for these analyses was that if the nature of the damage was a key factor in accounting for the observed FC changes, more damage would likely be associated with greater FC changes. However, contrary to this prediction, across these analyses we found little evidence of significant relationships between FC changes and the magnitude of structural damage (see Supplementary Material 4).

Second, we speculated that if the nature of the structural damage were critical in determining FC patterns, then the two groups would differ in their FC patterns more in the left hemisphere where the structural damage was concentrated. However, we found instead that the FC patterns for the two groups were more highly correlated in the heavily damaged left hemisphere and differed more in the right hemisphere (Figs. 5 and 6).

In sum, while these observations by no means fully address the possibility that differences in the focal/diffuse nature of the structural damage is the mechanism underlying the group differences in FC changes that we have reported, it is nonetheless the case that they do not especially support this hypothesis.

Temporal disease dynamics. Although increased homotopic FC synchronization and inter-hemispheric FC symmetry have not been specifically previously evaluated in PPA, in healthy aging and Alzheimer's Disease a loss of hemispheric specificity and greater "homogenization" of activation patterns have been proposed to be signature functional changes (Goh, 2011; Jones et al., 2011; Meinzer et al., 2009). Relatedly, symmetrical functional changes have been reported in PPA (Mandelli et al., 2018; Ranasinghe et al., 2017; Tao et al., 2020).

With regard to lifespan changes in lateralization of function, from childhood to adulthood brain areas supporting higher cognitive functions have been shown to become increasingly lateralized (Dehaene-Lambertz et al., 2018; Olulade et al., 2020), presumably reflecting functional specialization and neural differentiation. However, starting in later middle age this trend may reverse with more distributed and bilateral activation patterns (Cabeza, 2002; Meinzer et al., 2009) and increasing levels of inter-hemispheric synchronicity (Avelar-Pereira et al., 2020; Zuo et al., 2010). The reasons for this "re-emergence" of greater hemispheric symmetry in aging is debated. Some have proposed a general process of de-differentiation (Cabeza, 2002), while others,

including some working on preclinical Alzheimer's Disease, have suggested that some of these neural changes may be compensatory and precede overt behavioral decrements (for reviews see Hillary & Grafman, 2017; Stargardt et al., 2015). The fact that de-differentiation across the hemispheres has been observed both in progressive brain disease and healthy aging suggests that they might be a response to a gradual time-course of damage. In the context of progressive neurological disease, Desmurget et al. (2007) specifically speculated that these characteristics may be due to plasticity mediated by a gradual "supervised learning process" that allows for the reshaping of proximal and distal functional networks. With regard to behaviora consequence, they suggestthat, after a long pre-clinical period of changes that help maintain behavioral integrity, the gradual damage exceeds neuroplastic capacity and behavioral deficits emerge. Despite these intriguing similarities, the extent to which progressive neurological disease and aging share similar neoplastic changes and underlying disease kinetics is a topic that clearly merits further careful attention.

In terms of stroke, the increased FC asymmetry between the hemispheres that we found is consistent with other previous reports indicating that in post-stroke aphasia, the ipsi-lesional LH often shows hypo-connectivity while the RH often shows hyper-connectivity that may normalize or persist throughout the chronic period (Hartwigsen & Saur, 2019; Saur et al., 2006). These findings support the conclusion that after stroke, the contra-lesional hemisphere undergoes functional changes that are distinct from those that occur in the ipsi-lesional hemisphere. Interestingly, similar findings have also been reported in the context of tumor resection (Almairac et al., 2021; Coget et al., 2018). While tumor resection may typically occur following a more prolonged period of neural disruption than stroke, both stroke and resection include major, abrupt neurological changes. Thus, similarities in FC outcomes between the stroke and tumor resection support the hypothesis that abrupt, unilateral focal damage may trigger functional dissociations between the two hemispheres.

The location of structural damage. The two previous sections focused on possible explanations for the observed *differences* in the FC changes across the two groups. However, also potentially relevant to understanding underlying mechanisms are the similarities in FC changes that we observed. The fact that these changes were so similar in the heavily damaged left hemisphere (Fig. 6) suggests that neither the nature of the structural damage nor the different temporal disease trajectories can provide a full explanation. Instead, the patterns of similar FC changes across the groups seem likely to be the result of the location of the structural damage rather than factors related to damage etiology. In other words, the similar spatial damage distributions of the two groups produced similar FC changes. Because specific brain regions participate in specific functional and structural networks, their damage may trigger functional reorganization patterns that are independent of the nature of the damage. Examining other PSA and PPA groups with different damage epicenters (e.g., semantic and logopenic variant PPA) will be important for determining the extent to which the specific FC features we have observed in this study are linked to specific damage location or to the disease etiologies more generally.

In sum, while the available evidence regarding underlying mechanisms of the FC differences we have documented in stroke and neurodegenerative disease is very limited, it does suggest that the distinct functional changes of the two groups observed in the right-hemisphere and in inter-hemispheric relationships were not driven by the nature of the structural damage (diffuse vs focal). Instead, we have argued that disease time-course remains a viable hypothesis. However, as the spatial and temporal features are overlapping for the current two groups (i.e., abrupt disease onset and focal damage vs slow development and diffuse damage), it is extremely difficult to disentangle the two factors. Importantly the results do suggest that the location of damage is a relevant factor for understanding the FC similarities observed in the heavily damaged left hemisphere. Understanding the possible contributions and interactions between these factors clearly will require

further examination including, importantly, longitudinal studies of FC changes in diseases with different damage time-courses, damage types and damage locations.

5. Limitations

Limitations include that, within PPA, we examined only the non-fluent PPA variant. Examination of other PPA variants will be necessary to determine if the features we observed for PPA generalize across the disease or are restricted to the non-fluent variant. More generally, the study of additional diseases and conditions (e.g., anoxia, slow-growing tumors, vascular brain disease) will allow further disentangling of the contribution of damage type and disease trajectory. Finally, a more comprehensive and detailed examination of FC-behavior relationships would be very valuable, although it was clearly beyond the scope of this paper that was focused on documenting and describing robust FC changes. Despite the limited investigation of FC-behavior relationships, the fact that different patterns of homotopic FC changes in the two groups were associated with different cognitive functions (executive functions in PPA and language in PSA), does underscore the behavioral relevance of FC changes and provides some initial insights regarding the nature of the reorganization that results from the different neuropathologies.

6. Conclusions

In this study we identified shared and distinct features of the functional neuroplastic responses of two neuropathological conditions – stroke and neurodegenerative disease. We specifically examined two groups of individuals with post-stroke and progressive aphasia with regard to the two stroke phenotype features proposed by Siegel et al. (2016) – decreased inter-hemispheric functional connectivity (FC) and increased intra-hemispheric FC. We found that the two diseases differed from one another clearly and substantially regarding inter-hemispheric, homotopic FC. However, with regard to the second stroke phenotype feature we found that neither group provided a exhibited a consistent pattern of increased intra-hemispheric FC. We did find, however, that the two groups were strikingly similar in terms of their patterns of left hemisphere FC but differed in their FC patterns in the right hemisphere. Overall, we found that generally similar distributions of left hemisphere damage in the two etiologies resulted in similar functional connectivity changes within the left hemisphere. However, abrupt onset, focal disease produced greater independence in hemispheric responses, while a slowly developing diffuse damage resulted in more symmetrical changes across the hemispheres as well as more synchronized activity between them. These findings constitute novel evidence regarding the specific patterns of functional reorganization associated with stroke and neurodegenerative disease. They not only underscore the importance of disease location in shaping neuroplastic responses, they raise the possibility that the temporal time-course of damage progression may also play a significant role in the brain's response to damage.

CRediT authorship contribution statement

Yuan Tao: Conceptualization, Data curation, Formal analysis, Visualization. **Kyrana Tsapkini:** Funding acquisition, Supervision, Writing – review & editing. **Brenda Rapp:** Funding acquisition, Supervision, Writing – review & editing.

Declaration of Competing Interest

The authors declare that they have no known competing financial interests or personal relationships that could have appeared to influence the work reported in this paper.

Data availability

Data will be made available on request.

Appendix A. Supplementary data

Supplementary data to this article can be found online at https://doi.org/10.1016/j.nicl.2022.103263.

References

Agosta, F., Galantucci, S., Valsasina, P., Canu, E., Meani, A., Marcone, A., Magnani, G., Falini, A., Comi, G., Filippi, M., 2014. Disrupted brain connectome in semantic variant of primary progressive aphasia. Neurobiol. Aging 35 (11), 2646–2655. https://doi.org/10.1016/j.neurobiolaging.2014.05.017.

Almairac, F., Deverdun, J., Cochereau, J., Coget, A., Lemaitre, A.-L., Moritz-Gasser, S., Duffau, H., Herbet, G., 2021. Homotopic redistribution of functional connectivity in insula-centered diffuse low-grade glioma. NeuroImage: Clinical 29, 102571.

Anglade, C., Thiel, A., Ansaldo, A.I., 2014. The complementary role of the cerebral hemispheres in recovery from aphasia after stroke: a critical review of literature. Brain Inj. 28 (2), 138–145. https://doi.org/10.3109/02699052.2013.859734.

Avelar-Pereira, B., Bäckman, L., Wåhlin, A., Nyberg, L., Salami, A., 2020. Increased functional homotopy of the prefrontal cortex is associated with corpus callosum degeneration and working memory decline. Neurobiol. Aging 96, 68–78. https://doi.org/10.1016/j.neurobiolaging.2020.08.008.

Army Individual Test Battery. (1944). *Manual of directions and scoring.* War Department, Adjutant General's Office.

Bonakdarpour, B., Hurley, R.S., Wang, A.R., Fereira, H.R., Basu, A., Chatrathi, A., Guillaume, K., Rogalski, E.J., Mesulam, M.M., 2019. Perturbations of language network connectivity in primary progressive aphasia. Cortex 121, 468–480. https://doi.org/10.1016/j.cortex.2019.08.010.

Brodtmann, A., Khlif, M.S., Egorova, N., Veldsman, M., Bird, L.J., Werden, E., 2020. Dynamic regional brain atrophy rates in the first year after ischemic stroke. Stroke 51 (9). https://doi.org/10.1161/STROKEAHA.120.030256.

Cabeza, R., 2002. Hemispheric asymmetry reduction in older adults: the HAROLD model. Psychol. Aging 17 (1), 85–100. https://doi.org/10.1037/0882-7974.17.1.85.

Cao, Y., Vikingstad, E.M., George, K.P., Johnson, A.F., Welch, K.M.A., 1999. Cortical language activation in stroke patients recovering from aphasia with functional MRI. Stroke 30 (11), 2331–2340. https://doi.org/10.1161/01.STR.30.11.2331.

Coget, A., Deverdun, J., Bonafé, A., van Dokkum, L., Duffau, H., Molino, F., Le Bars, E., de Champfleur, N., 2018. Transient immediate postoperative homotopic functional disconnectivity in low-grade glioma patients. NeuroImage: Clinical 18 (August 2017), 656–662. https://doi.org/10.1016/j.nicl.2018.02.023.

Crofts, J.J., Higham, D.J., Bosnell, R., Jbabdi, S., Matthews, P.M., Behrens, T.E.J., Johansen-Berg, H., 2011. Network analysis detects changes in the contralesional hemisphere following stroke. NeuroImage 54 (1), 161–169. https://doi.org/10.1016/j.neuroimage.2010.08.032.

Dehaene-Lambertz, G., Monzalvo, K., Dehaene, S., 2018. The emergence of the visual word form: Longitudinal evolution of category-specific ventral visual areas during reading acquisition. *PLoS Biol.* 16 (3) https://doi.org/10.1371/journal.pbio.2004103.

Desmurget, M., Bonnetblanc, F., Duffau, H., 2007. Contrasting acute and slow-growing lesions: a new door to brain plasticity. Brain 130 (4), 898–914. https://doi.org/10.1093/brain/awl300.

Douaud, G., Smith, S., Jenkinson, M., Behrens, T., Johansen-Berg, H., Vickers, J., James, S., Voets, N., Watkins, K., Matthews, P.M., James, A., 2007. Anatomically related grey and white matter abnormalities in adolescent-onset schizophrenia. Brain 130 (9), 2375–2386. https://doi.org/10.1093/brain/awm184.

Egorova-Brumley, N., Khlif, M.S., Werden, E., Bird, L.J., Brodtmann, A., 2022. Grey and white matter atrophy 1 year after stroke aphasia. Brain Commun. 4 (2) https://doi.org/10.1093/braincomms/fcac061.

Fornito, A., Zalesky, A., Pantelis, C., Bullmore, E.T., 2012. Schizophrenia, neuroimaging and connectomics. NeuroImage 62 (4), 2296–2314. https://doi.org/10.1016/j.neuroimage.2011.12.090.

Gainotti, G., 2015. Contrasting opinions on the role of the right hemisphere in the recovery of language. A critical survey. *Aphasiology* 29 (9), 1020–1037. https://doi.org/10.1080/02687038.2015.1027170.

Goh, J.O.S., 2011. Functional dedifferentiation and altered connectivity in older adults: neural accounts of cognitive aging. Aging Dis. 2 (1), 30–48.

Gorno-Tempini, M.L., Hillis, A.E., Weintraub, S., Kertesz, A., Mendez, M., Cappa, S.F., Ogar, J.M., Rohrer, J.D., Black, S., Boeve, B.F., Manes, F., Dronkers, N.F., Vandenberghe, R., Rascovsky, K., Patterson, K., Miller, B.L., Knopman, D.S., Hodges, J.R., Mesulam, M.M., Grossman, M., 2011. Classification of primary progressive aphasia and its variants. Neurology 76 (11), 1006–1014. https://doi.org/10.1212/WNL.0b013e31821103e6.

Guo, C.C., Gorno-Tempini, M.L., Gesierich, B., Henry, M., Trujillo, A., Shany-Ur, T., Jovicich, J., Robinson, S.D., Kramer, J.H., Rankin, K.P., Miller, B.L., Seeley, W.W., 2013. Anterior temporal lobe degeneration produces widespread network-driven dysfunction. Brain 136 (10), 2979–2991. https://doi.org/10.1093/brain/awt222.

Hartwigsen, G., Saur, D., 2019. Neuroimaging of stroke recovery from aphasia – Insights into plasticity of the human language network. NeuroImage 190 (November), 14–31. https://doi.org/10.1016/j.neuroimage.2017.11.056.

Hillary, F.G., Grafman, J.H., 2017. Injured brains and adaptive networks: the benefits and costs of hyperconnectivity. Trends Cogn. Sci. 21 (5), 385–401. https://doi.org/10.1016/j.tics.2017.03.003.

Ingram, R.U., Halai, A.D., Pobric, G., Sajjadi, S., Patterson, K., Lambon Ralph, M.A., 2020. Graded, multidimensional intra- and intergroup variations in primary progressive aphasia and post-stroke aphasia. Brain 143 (10), 3121–3135. https://doi.org/10.1093/brain/awaa245.

Joliot, M., Jobard, G., Naveau, M., Delcroix, N., Petit, L., Zago, L., Crivello, F., Mellet, E., Mazoyer, B., Tzourio-Mazoyer, N., 2015. AICHA: An atlas of intrinsic connectivity of homotopic areas. J. Neurosci. Methods 254, 46–59. https://doi.org/10.1016/j.jneumeth.2015.07.013.

Jones, D.T., MacHulda, M.M., Vemuri, P., McDade, E.M., Zeng, G., Senjem, M.L., Gunter, J.L., Przybelski, S.A., Avula, R.T., Knopman, D.S., Boeve, B.F., Petersen, R.C., Jack, C.R., 2011. Age-related changes in the default mode network are more advanced in Alzheimer disease. Neurology 77 (16), 1524–1531. https://doi.org/10.1212/WNL.0b013e318233b33d.

Kertesz, A. (2006). *Western Aphasia Battery – Revised*. https://doi.org/https://doi.org/10.1037/t15168-000.

Klingbeil, J., Wawrzyniak, M., Stockert, A., Saur, D., 2019. Resting-state functional connectivity: an emerging method for the study of language networks in post-stroke aphasia. Brain Cogn. 131 (March), 22–33. https://doi.org/10.1016/j.bandc.2017.08.005.

Knopman, D.S., Kramer, J.H., Boeve, B.F., Caselli, R.J., Graff-Radford, N.R., Mendez, M.F., Miller, B.L., Mercaldo, N., 2008. Development of methodology for conducting clinical trials in frontotemporal lobar degeneration. Brain 131 (11), 2957–2968. https://doi.org/10.1093/brain/awn234.

Lehmann, M., Madison, C., Ghosh, P.M., Miller, Z.A., Greicius, M.D., Kramer, J.H., Coppola, G., Miller, B.L., Jagust, W.J., Gorno-Tempini, M.L., Seeley, W.W., Rabinovici, G.D., 2015. Loss of functional connectivity is greater outside the default mode network in nonfamilial early-onset Alzheimer's disease variants. Neurobiol. Aging 36 (10), 2678–2686. https://doi.org/10.1016/j.neurobiolaging.2015.06.029.

Mandelli, M.L., Welch, A.E., Vilaplana, E., Watson, C., Battistella, G., Brown, J.A., Possin, K.L., Hubbard, H.I., Miller, Z.A., Henry, M.L., Marx, G.A., Santos-Santos, M.A., Bajorek, L.P., Fortea, J., Boxer, A., Rabinovici, G., Lee, S., Deleon, J., Rosen, H.J., Miller, B.L., Seeley, W.W., Gorno-Tempini, M.L., 2018. Altered topology of the functional speech production network in non-fluent/agrammatic variant of PPA. Cortex 108, 252–264.

Meinzer, M., Flaisch, T., Wilser, L., Eulitz, C., Rockstroh, B., Conway, T., Gonzalez-Rothi, L., Crosson, B., 2009. Neural signatures of semantic and phonemic fluency in young and old adults. J. Cognit. Neurosci. 21 (10), 2007–2018. https://doi.org/10.1162/jocn.2009.21219.

Nooner, K.B., Colcombe, S.J., Tobe, R.H., Mennes, M., Benedict, M.M., Moreno, A.L., Panek, L.J., Brown, S., Zavitz, S.T., Li, Q., Sikka, S., Gutman, D., Bangaru, S., Schlachter, R.T., Kamiel, S.M., Anwar, A.R., Hinz, C.M., Kaplan, M.S., Rachlin, A.B., Adelsberg, S., Cheung, B., Khanuja, R., Yan, C., Craddock, C.C., Calhoun, V., Courtney, W., King, M., Wood, D., Cox, C.L., Kelly, A.M.C., Di Martino, A., Petkova, E., Reiss, P.T., Duan, N., Thomsen, D., Biswal, B., Coffey, B., Hoptman, M.J., Javitt, D.C., Pomara, N., Sidtis, J.J., Koplewicz, H.S., Castellanos, F.X., Leventhal, B.L., Milham, M.P., 2012. The NKI-Rockland sample: a model for accelerating the pace of discovery science in psychiatry. Front. Neurosci. 6 https://doi.org/10.3389/fnins.2012.00152.

Olulade, O.A., Seydell-Greenwald, A., Chambers, C.E., Turkeltaub, P.E., Dromerick, A.W., Berl, M.M., Gaillard, W.D., Newport, E.L., 2020. The neural basis of language development: changes in lateralization over age. Proc. Natl. Acad. Sci. USA 117 (38), 23477–23483. https://doi.org/10.1073/pnas.1905590117.

Patrissi, G., Stein, D.G., 1975. Temporal factors in recovery of function after brain damage. Exp. Neurol. 47 (3), 470–480. https://doi.org/10.1016/0014-4886(75)90079-5.

Power, J.D., Cohen, A.L., Nelson, S.M., Wig, G.S., Barnes, K.A., Church, J.A., Vogel, A.C., Laumann, T.O., Miezin, F.M., Schlaggar, B.L., Petersen, S.E., 2011. Functional network organization of the human brain. Neuron 72 (4), 665–678. https://doi.org/10.1016/j.neuron.2011.09.006.

Prabhakaran, V., Smith, J.A.L., Desmond, J.E., Glover, G.H., Gabrieli, J.D.E., 1997. Neural substrates of fluid reasoning: An fMRI study of neocortical activation during performance of the Raven's Progressive Matrices Test. Cogn. Psychol. 33 (1), 43–63. https://doi.org/10.1006/cogp.1997.0659.

Pruim, R.H.R., Mennes, M., van Rooij, D., Llera, A., Buitelaar, J.K., Beckmann, C.F., 2015. ICA-AROMA: a robust ICA-based strategy for removing motion artifacts from fMRI data. NeuroImage 112, 267–277. https://doi.org/10.1016/j.neuroimage.2015.02.064.

Ranasinghe, K.G., Hinkley, L.B., Beagle, A.J., Mizuiri, D., Honma, S.M., Welch, A.E., Hubbard, I., Mandelli, M.L., Miller, Z.A., Garrett, C., La, A., Boxer, A.L., Houde, J.F., Miller, B.L., Vossel, K.A., Gorno-Tempini, M.L., Nagarajan, S.S., 2017. Distinct spatiotemporal patterns of neuronal functional connectivity in primary progressive aphasia variants. Brain 140 (10), 2737–2751. https://doi.org/10.1093/brain/awx217.

Rao, K.V., Baddeley, A., 2013. Raven's matrices and working memory: a dual-task approach. Quart. J. Exp. Psychol. 66 (10), 1881–1887. https://doi.org/10.1080/17470218.2013.828314.

Raven, J.C., 1941. STANDARDIZATION OF PROGRESSIVE MATRICES, 1938. Br. J. Med. Psychol. 19 (1), 137–150. https://doi.org/10.1111/j.2044-8341.1941.tb00316.x.

Rogalski, E., Cobia, D., Harrison, T.M., Wieneke, C., Weintraub, S., Mesulam, M.M., 2011. Progression of language decline and cortical atrophy in subtypes of primary progressive aphasia. Neurology 76 (21), 1804–1810. https://doi.org/10.1212/WNL.0b013e31821ccd3c.

Sale, M.V., Mattingley, J.B., Zalesky, A., Cocchi, L., 2015. Imaging human brain networks to improve the clinical efficacy of non-invasive brain stimulation. Neurosci. Biobehav. Rev. 57, 187–198. https://doi.org/10.1016/j.neubiorev.2015.09.010.

Sánchez-Cubillo, I., Periáñez, J.A., Adrover-Roig, D., Rodríguez-Sánchez, J.M., Ríos-Lago, M., Tirapu, J., Barceló, F., 2009. Construct validity of the Trail Making Test: Role of task-switching, working memory, inhibition/interference control, and visuomotor abilities. J. Int. Neuropsychol. Soc. 15 (3), 438–450. https://doi.org/10.1017/S1355617709090626.

Saur, D., Lange, R., Baumgaertner, A., Schrakneppfer, V., Willmes, K., Rijntjes, M., Weiller, C., 2006. Dynamics of language reorganization after stroke. Brain 129 (6), 1371–1384. https://doi.org/10.1093/brain/awl090.

Siegel, J.S., Ramsey, L.E., Snyder, A.Z., Metcalf, N.V., Chacko, R.V., Weinberger, K., Baldassarre, A., Hacker, C.D., Shulman, G.L., Corbetta, M., 2016. Disruptions of network connectivity predict impairment in multiple behavioral domains after stroke. Proc. Natl. Acad. Sci. 113 (30), E4367–E4376. https://doi.org/10.1073/pnas.1521083113.

Siegel, J.S., Seitzman, B.A., Ramsey, L.E., Ortega, M., Gordon, E.M., Dosenbach, N.U.F., Petersen, S.E., Shulman, G.L., Corbetta, M., 2018. Re-emergence of modular brain networks in stroke recovery. Cortex 101, 44–59. https://doi.org/10.1016/j.cortex.2017.12.019.

Stam, C.J., Hillebrand, A., Wang, H., Van Mieghem, P., 2010. Emergence of modular structure in a large-scale brain network with interactions between dynamics and connectivity. Front. Comput. Neurosci. 4 (September), 1–13. https://doi.org/10.3389/fncom.2010.00133.

Stargardt, A., Swaab, D.F., Bossers, K., 2015. The storm before the quiet: Neuronal hyperactivity and Aβ in the presymptomatic stages of Alzheimer's disease. Neurobiol. Aging 36 (1), 1–11. https://doi.org/10.1016/j.neurobiolaging.2014.08.014.

Stein, D.G., Butters, N., Rosen, J., 1977. PERFORMANCE. 15, 179–182.

Tao, Y., Ficek, B., Rapp, B., Tsapkini, K., 2020. Different patterns of functional network reorganization across the variants of primary progressive aphasia: a graph-theoretic analysis. Neurobiol. Aging 96, 184–196. https://doi.org/10.1016/j.neurobiolaging.2020.09.007.

Tao, Y., Ficek, B., Wang, Z., Rapp, B., Tsapkini, K., 2021. Selective functional network changes following tDCS-augmented language treatment in primary progressive aphasia. Front. Aging Neurosci. 13 https://doi.org/10.3389/fnagi.2021.681043.

Tao, Y., Rapp, B., 2019. The effects of lesion and treatment-related recovery on functional network modularity in post-stroke dysgraphia. NeuroImage: Clin. 23, 101865.

Tao, Y., Rapp, B., 2020. How functional network connectivity changes as a result of lesion and recovery: an investigation of the network phenotype of stroke. Cortex 131, 17–41. https://doi.org/10.1016/j.cortex.2020.06.011.

Thulborn, K.R., Carpenter, P.A., Just, M.A., 1999. Plasticity of language-related brain function during recovery from stroke. Stroke 30 (4), 749–754. https://doi.org/10.1161/01.STR.30.4.749.

Turkeltaub, P.E., 2015. Brain stimulation and the role of the right hemisphere in aphasia recovery. Curr. Neurol. Neurosci. Rep. 15 (11) https://doi.org/10.1007/s11910-015-0593-6.

Turkeltaub, P.E., Messing, S., Norise, C., Hamilton, R.H., 2011. Are networks for residual language function and recovery consistent across aphasic patients? Neurology 76 (20), 1726–1734. https://doi.org/10.1212/WNL.0b013e31821a44c1.

van Wijk, B.C.M., Stam, C.J., Daffertshofer, A., Sporns, O., 2010. Comparing brain networks of different size and connectivity density using graph theory. PLoS One 5 (10), e13701. https://doi.org/10.1371/journal.pone.0013701.

Whitwell, J.L., Jones, D.T., Duffy, J.R., Strand, E.A., Machulda, M.M., Przybelski, S.A., Vemuri, P., Gregg, B.E., Gunter, J.L., Senjem, M.L., Petersen, R.C., Jack, C.R., Josephs, K.A., 2015. Working memory and language network dysfunctions in logopenic aphasia: a task-free fMRI comparison with Alzheimer's dementia. Neurobiol. Aging 36 (3), 1245–1252. https://doi.org/10.1016/j.neurobiolaging.2014.12.013.

Zuo, X.N., Kelly, C., Di Martino, A., Mennes, M., Margulies, D.S., Bangaru, S., Grzadzinski, R., Evans, A.C., Zang, Y.F., Castellanos, F.X., Milham, M.P., 2010. Growing together and growing apart: regional and sex differences in the lifespan developmental trajectories of functional homotopy. J. Neurosci. 30 (45), 15034–15043. https://doi.org/10.1523/JNEUROSCI.2612-10.2010.